

**Enhancement of the Epitopic Activity of Anti-Thrombotic
Peptidomimetics by Conjugation to a Macromolecular Carrier**

by

JERRY GONGDU ZHANG

B.Sc. (Honours.), The University of British Columbia, 2007

**A THESIS SUBMITTED IN PARTIAL FULFILLMENT OF THE
REQUIREMENTS FOR THE DEGREE OF**

MASTER OF SCIENCE

In

THE FACULTY OF GRADUATE STUDIES

(Pathology and Laboratory Medicine)

THE UNIVERSITY OF BRITISH COLUMBIA

(Vancouver)

July 2008

©Jerry Gongdu Zhang, 2008

Abstract

Background: Novel peptides with epitopic activity can be discovered by a combination of peptide arrays and computational interpolation. These peptides can mimic the activity of cellular receptors or their ligands, and are thus called peptidomimetics. The activity of peptidomimetics evidently varies in accordance with the attributes of the peptide. The fibrin-mimetic, Arginine-Glycine-Aspartate (RGD), is a well known anti-thrombotic peptide which inhibits the interaction between the platelet integrin GPIIbIIIa and fibrinogen/fibrin. Short peptides often suffer from high inhibitory concentrations *in vitro* and short clearance times *in vivo*. To increase vascular residence times of such antithrombotic peptides, they were coupled to macromolecular carriers. Hyperbranched polyglycerols (HPG), macromolecules designed as a dendritic carrier species, at a range of HPG molecular weights (MW) were tested as the carriers for antithrombotic peptidomimetics.

Methods: HPG of MW 3 to 500 kDa were conjugated with RGD at a range of substitution ratios. The optimum molecular weight and substitution ratio were then applied to the peptide SHAYIGLKDR, a vWf mimic peptide discovered through the use of bioinformatics. For peptidomimetics (RGD and SHAYIGLKDR), enzymatic proteolysis was employed to distinguish the specificity of the inhibitory activity among HPG, peptide, and the HPG-peptide conjugate. Flow cytometry, UV spectroscopy, compound light microscopy, and lumiaggregometry were used to characterize the function of the conjugates *in vitro*.

Results: Conjugation of RGD to HPG resulted in a decrease of the inhibitory concentration required to interrupt platelet-fibrinogen interactions by up to three orders of magnitude. Inhibitory activity was directly related to the number of peptides attached per HPG. Similar results were found when high molecular weight HPG, selected from the RGD-related experiments, was used to carry the peptide SHAYIGLKDR. None of HPG, RGD, SHAYIGLKDR, or their conjugates caused spontaneous platelet activation, or inhibited thrombin-mediated platelet activation, showing that the peptides' activity is directed specifically toward their targets: GPIIb/IIIa/fibrinogen (RGD) and GPIb/vWf (SHAYIGLKDR) interactions. Tryptic digestion of conjugates confirmed that the inhibitory activity of HPG conjugates was dependent on the presence of the intact peptides.

Conclusions: Conjugation of peptidomimetics or other molecules to macromolecular platforms such as HPG is a viable method to enhance the peptidomimetics' activity. The degree of enhancement is dependent upon the level of peptide substitution as well as the size of the carrier.

Table of Contents

Abstract.....	ii
Table of Contents.....	iv
List of Tables.....	vi
List of Figures.....	vii
List of Abbreviations.....	ix
Acknowledgements.....	x
CHAPTER 1. Introduction.....	1
1.1 General Platelet Characteristics and Function.....	1
1.2 Platelet Integrins and Mechanism of Action.....	3
1.3 Anti-thrombotics.....	7
1.4 Peptidomimetics.....	10
1.5 Macromolecular Carriers and Conjugation.....	14
1.6 Peptide Polarity and Chirality.....	18
1.7 Hypothesis.....	21
CHAPTER 2. Materials and Methods.....	23
2.1 Peptides and Proteins.....	23
2.2 Preparation of Human Platelets.....	23
2.3 HPG-RGD Conjugates.....	24
2.4 HPG-SHAYIGLKDR Conjugates.....	28
CHAPTER 3. Results.....	35
3.1 HPG-RGD Conjugates.....	35
3.2 HPG-SHAYIGLKDR Conjugates.....	45
CHAPTER 4. Discussion.....	52
4.1 HPG-RGD Conjugates.....	52
4.2 HPG-SHAYIGLKDR Conjugates.....	57
4.3 Summary.....	61
CHAPTER 5. Conclusion.....	63

Bibliography.....	65
Appendices.....	72
Appendix A.....	72

List of Tables

Table 3.11	Synthesis, characterization, and evaluation of RGD and RGD-HPG conjugates.....	36
Table 3.12	Light microscopy of RGD-HPG conjugates and aggregation of resting and Mn^{2+} activated platelets in the presence of free RGD peptides and RGD-HPG conjugates at their respective I_{C50} values.....	41
Table 3.21	Functionalization and Characterization of HPG and HPG Conjugates.....	46
Table 3.22	Light microscopy, aggregometry, and flow cytometry of HPG-conjugates with resting and/or activated platelets.....	46

List of Figures

Figure 1.11	Platelet-Platelet and Platelet-Subendothelium Interactions During Thrombosis.....	2
Figure 1.21	Platelet Activation Signalling Pathways.....	6
Figure 1.31	Conventional Antithrombotics and Their Targets in Platelet Signalling Pathways.....	9
Figure 1.41	MLAX Interpolated vWf Peptidomimetic (SHAYIGLKDR) Inhibition of GPIb-vWf Interaction.....	12
Figure 1.51	Carrier Valency.....	15
Figure 1.52	Relationship Between Linker Length and Degrees of Freedom in High Density Brushes.....	16
Figure 1.61	Nomenclature of Peptide Polarity.....	19
Figure 1.62	The SHAYIGLKDR Peptide and its D-Enantiomer.....	20
Figure 2.31	Functionalization of HPG and Conjugation of RGD Peptides.....	25
Figure 2.41	Functionalization of HPG and Conjugation of SHAYIGLKDR Peptides....	30
Figure 3.12	Evaluation of the Effect of Unconjugated HPGs on Resting and Activated Platelets.....	37
Figure 3.13.1	Effect of HPG-RGD Conjugates on Fibrinogen Binding by Resting Platelets.....	38
Figure 3.13.2	Trypsin Proteolysis Assay of RGD and HPG-RGD Conjugates.....	39
Figure 3.14	Inhibitory Effects of HPG-RGD Conjugates on Platelet-Fibrinogen Binding.....	42
Figure 3.15	Relationships Among I_{c50} , HPG Polymer Molecular Weight and Amount of RGD Peptides Conjugated to HPG.....	43
Figure 3.16	Light Microscopy and Aggregometry.....	44
Figure 3.23.1	Inhibition of Platelet-vWf Binding by Peptide-conjugated HPG.....	49
Figure 3.23.2	Trypsin Proteolysis Assay of SHAYIGLKDR and HPG-SHAYIGLKDR Conjugates.....	50

Figure 3.23.3	Effect of Peptide on GPIIb/IIIa Activation Through GPIb Signalling.....	51
Figure 4.11	Proposed Mechanism A: Polyvalency of HPG-RGD Conjugates.....	55
Figure 4.12	Proposed Mechanism B: Higher Local Concentration.....	56

List of Abbreviations

DVS = Divinyl sulfone

GPIb-IX-V = Glycoprotein Ib/IX/V integrin complex

GPIIbIIIa = Glycoprotein IIb/IIIa integrin complex

HPG = Hyperbranched Polyglycerols

I_{C50} = Inhibitory Concentration, a concentration at which 50% inhibition is achieved

M_n = Number Average Molecular Weight

M_w = Weight Average Molecular Weight

MW = Molecular weight

PAR = Platelet activated receptor

PDI = Polydispersity

PEG = Polyethylene Glycol

PI = Phosphoinositol

RGD = Arginine-Glycine-Aspartic Acid

SBTI = Soybean Trypsin Inhibitor

SHAYIGLKDR = polypeptide Serine-Histidine-Alanine-Tyrosine-Isoleucine-Glycine-Leucine-Lysine-Aspartic Acid-Arginine

TP = Thromboxane/prostanoid receptor

VS = Vinyl sulfone

vWf = von Willebrand Factor

Acknowledgements

I would like to thank Canadian Blood Services, Canadian Institutes of Health Research, NSERC, the Canadian Foundation for Innovation, the Heart and Stroke Foundation of Canada, and the UBC Centre for Blood Research for their funding support of this project and its personnel.

People with experimental contributions are gratefully acknowledged: Dr. Rajesh Kainthan produced all HPG molecules of varying molecular weights, and all HPG-RGD conjugates. Dr. William Campbell produced the vWf sequence peptide array from which we derived the preliminary vWf peptidomimetics and Dr. Carlos Del Carpio used MIAx bioinformatics software to narrow down our selections of those peptides. Mr. Oren B. Kraiden performed the preliminary tests on the HPG-RGD conjugates and Ms. Wendy W.Y. Lin contributed to the establishment of the ristocetin-vWf mediated platelet activation assays in flow cytometry, microscopy, and aggregometry.

I would like to further acknowledge the people of Canadian Blood Services Devine-Issa Lab: Peter Shubert, Iren Constantinescu, Katherine Serrano, Elena Levin, and Brankica Culibrk for their assistance with my experiments. Finally, I would like to thank my research supervisor, Dr. Maria Gyongyossy-Issa, without whose source of crazy ideas, awesome support, and endless cat-sitting chores, these projects and this thesis could never have materialized.

No graduate students were badly harmed in the production of this thesis.

Chapter 1 – Introduction

1.1 General Platelet Characteristics and Function

Platelets are anucleate cell fragments of megakaryocytes, 1-2 μm in diameter (Kaushansky, 2005). Platelets enclose a complement of secretory granules: α -granules contain thrombospondin, von Willebrand Factor (vWf), coagulation factors, fibrinogen, ADP, P-selectin; and dense granules contain ADP/ATP, Ca^{2+} , histamines, serotonin, and epinephrine; though the majority of compounds/proteins in these granules have not been identified (Coppinger & Maguire, 2007). The contents of these granules mediate thrombosis and vascular repair through extensive signalling mechanisms involving endothelial cells, leukocytes, plasma proteins, and the platelets themselves. The primary function of platelets is to participate in thrombus formation by anchoring through Glycoprotein Ib-vWf (Varga-Szabo *et al.*, 2008) to collagen exposed on the damaged subendothelium and cross-linking each other through Glycoprotein IIb/IIIa-fibrin(ogen) (Varga-Szabo *et al.*, 2008). The consequent release of cytokines and chemokines signal other platelets (Coppinger & Maguire, 2007), and interact with polymerized fibrin fibrils to perform clot retraction (Mosesson, 2007; Weyrich *et al.*, 2007). To realize these functions, platelets are also highly amoeboid: cytoskeletal remodelling of actin allows platelets to assume a variety of shapes both for motility and during activation (Bearer *et al.*, 2002). Although platelets do not contain nuclei, regulation and control of cytoplasmic proteins is thought to be controlled by translation of innate mRNA, inherited from megakaryocytes (Weyrich *et al.*, 2007). Platelets have a maximum *in vivo* lifespan of 9-11 days before apoptosis mechanisms are triggered, but they may be cleared by

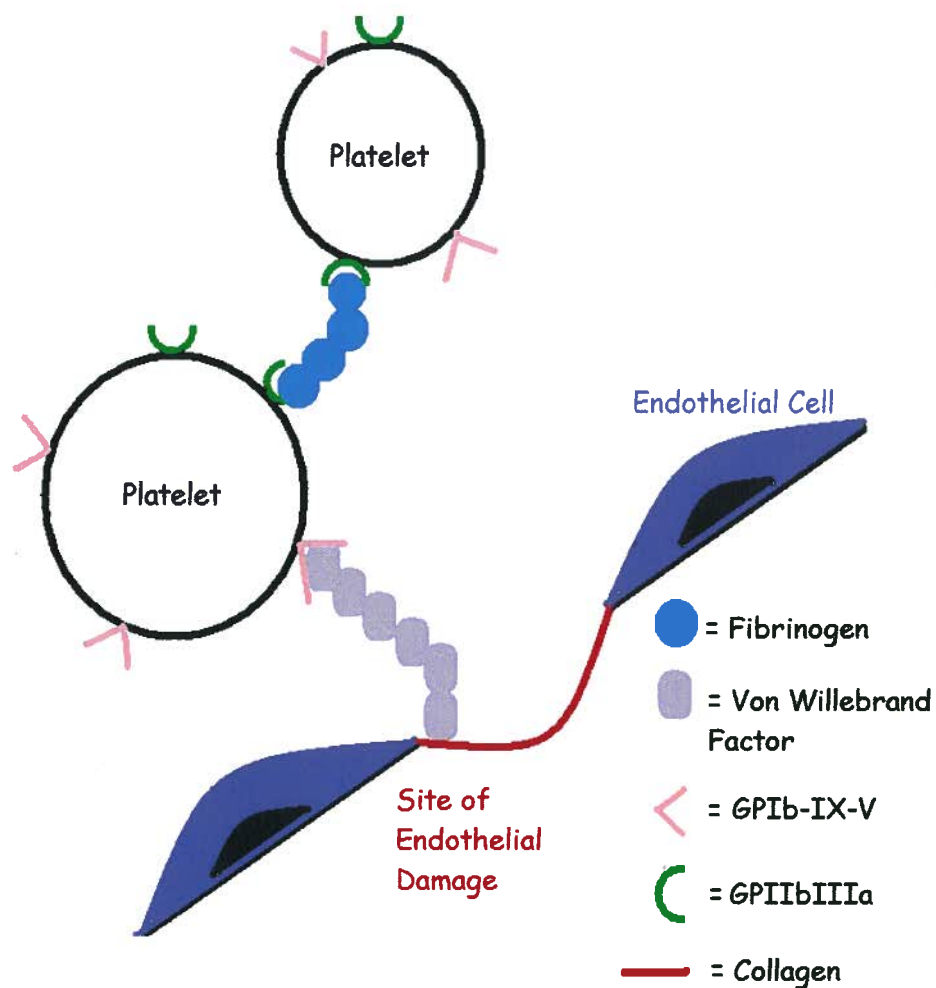


Figure 1.11 Platelet-platelet and Platelet-subendothelium Interactions During Thrombosis. Platelets are cross-linked by interaction of GPIIb/IIIa with polymerized fibrinogen/fibrin fibrils and anchored to the site of damage by interaction of GPIb and vWf to exposed collagen.

macrophages before this time due to a steady basal level of activation stimulus experienced during circulation (Mason *et al.*, 2007).

1.2 Platelet Integrins and Mechanism of Activation

Platelet activation and thrombus formation are initiated by signalling pathways rooted in the cell-surface integrin receptors and the receptors' binding of their ligands (Gibbins, 2004; Calvete, 2004; Du 2006; Figure 1.2). Several such receptors and their respective ligands are particularly important: GPIb with vWf; PAR1/PAR4, P₂Y₁/P₂Y₁₂, TP receptors with soluble antagonists thrombin, ADP, and thromboxane A₂; GPIIb/IIIa - fibrinogen/fibrin. Platelet activation can be triggered through mechanisms related to these integrins (Shattil & Newman, 2004).

Probably the initial activation mechanism is through von Willebrand factor. Conditions of high hydrodynamic shear, often induced by endothelial damage, activate vWf (250 kDa) in the plasma (Ruggeri, 2007). vWf will spontaneously bind to collagen, which is only exposed where there is endothelial damage (Andrews *et al.*, 1997; Lopez & Dong, 2005; Ruggeri, 2007). Activation of vWf by conformational change (Andrews *et al.*, 1997; Ruggeri, 2007) exposes the A1-domain, which will cause vWf to bind to the platelet surface integrin GPIb-IX-V complex (Lopez & Dong, 2005; Varga-Szabo *et al.*, 2008). This binding induces conformational changes of the integrin complex that trigger tyrosine kinases attached to the cytoplasmic portion of GPIb. In turn, these kinases trigger PKG and phospholipase C activation (Yin *et al.*, 2008), resulting in platelet activation by degranulation of the cytokine/chemokine containing α -granules and dense

granules, and result in the collateral activation of GPIIb/IIIa to the active conformation (Gibbins, 2004; Beer *et al.*, 1992).

A subsequent mechanism of platelet activation is also thought to function during the amplification of the platelet activation cascade and is triggered by soluble agonists (Dawood *et al.*, 2007). These agonists are stored in platelet α -granules and include ADP, thromboxane A_2 and platelet-derived thrombin and they are used in an autocrine/paracrine manner by platelets to stimulate the surface integrins (Dawood *et al.*, 2007; Vilahur *et al.*, 2007). Integrins activated by these cytokines include PAR1, PAR4, P_2Y_1 , P_2Y_{12} , and TP. These receptors are involved in platelet aggregation, PI-3 kinase activation, Ca^{2+} influx, and phospholipase C activation, which all lead to iterative degranulation and activation of GPIIb/IIIa to the active conformation (Dubois *et al.*, 2004; Du, 2007).

Another of these activation mechanisms is dependent upon thrombin (Factor IIa), which is the end target for activation of the coagulation cascade (Green, 2006). Thrombin cleaves fibrinogen into fibrin, which polymerizes and binds to platelet GPIIb/IIIa in its open conformation (Kasirer-Friede *et al.*, 2001). This interaction causes Ca^{2+} influx and phospholipase C activation, which again leads to platelet activation by degranulation. Fibrinogen binding to platelet GPIIb/IIIa induces a conformation change of the integrin such that signal transduction leads to Ca^{2+} influx into the platelet, which triggers further degranulation (Watson *et al.*, 2005; Du, 2007).

It should be noted that thrombin interacts with a variety of platelet integrins including GPIb, GPIIb/IIIa, PAR1/PAR4, etc. Thrombin binding may enhance ligand binding or help localize fibrin generation to platelet surfaces (GPIb), or may serve to

induce platelet activation by direct interaction with those integrins (PAR receptors) (Dubois *et al.*, 2004; Du, 2007).

All of these pathways result in the release of α -granule contents and the exposure of P-selectin (CD62) on platelet surfaces, which allow platelets to attach to endothelial cells (Jurk & Kehrel, 2005) and leukocytes (McGregor *et al.*, 2006) and initiate a rolling mechanic also observed for leukocytes. Hence CD62 surface expression is often considered a global sign of platelet activation – it is a sign that one or more of the above mentioned mechanisms has been triggered. Other ways to evaluate platelet activation also include platelet-fibrinogen binding, and platelet-vWf binding.

It is useful to note that independent of the coagulation cascade, which produces thrombin from plasma-derived prothrombin, platelet activation is a step-wise process. Platelet GPIb binds activated vWf, the platelet degranulates and rolls along the endothelium, the cytokines and chemokines released by platelets during degranulation trigger further degranulation and activate GPIIb/IIIa. GPIIb/IIIa binds fibrinogen/fibrin and further facilitates platelet activation. Eventually platelets will roll into the damaged site and be anchored to collagen by the other end of vWf multimers, and as more and more thrombin as well as platelets accumulate, platelets become cross-linked by fibrin fibrils through their activated GPIIb/IIIa receptors, and a thrombus is formed. Further thrombus refinement such as clot retraction occurs within hours of initial thrombus formation (Zimmerman & Weyrich, 2008). Hence, GPIb-vWf interaction is often considered to be upstream of most platelet activation mechanisms, a potentially useful target for clinical applications (Clementson & Clementson 2008).

1.3 Antithrombotics

Antithrombotics are a series of inhibitors aimed at mitigating the coagulation cascade, platelet activation, platelet attachment to the endothelium, and subsequent thrombus formation (Vanhoorelbeke *et al.*, 2003; Clementson & Clementson 2008). Due to the complexity of coagulation and thrombosis, many drugs exist which target different aspects of thrombus formation. These drugs can be categorized with respect to their effect on the coagulation cascade or platelet activation: vitamin K antagonists, anti-thrombin III enhancers, GPIIb/IIIa inhibitors, platelet aggregation inhibitors, plasminogen activators, direct thrombin inhibitors, and non-specific chemical compounds (Figure 1.31), inhibitors of the thromboxane/prostanoid receptor; P2Y₁/P2Y₁₂: G-coupled receptors of the P2Y nucleotide-sensing family (Du, 2006).

Vitamin K antagonists interfere with vitamin K dependent synthesis of clotting factors II (thrombin), VII, IX, X, and in turn disrupt the coagulation cascade, preventing fibrin generation and platelet cross-linking (Merli & Fink, 2008); classic examples include warfarin and Fluindione™ (Bossavy *et al.*, 1999). Anti-thrombin enhancers bind to anti-thrombin and increase its affinity to thrombin by inducing slight conformational changes, resulting in reduced active thrombin and lowered platelet activation as well as reduced fibrin generation (Selwyn, 2003); heparin is a classical example of such a compound (Bjork & Lindahl, 1982; McRae & Ginsberg, 2005; Prandoni *et al.* 2008). GPIIbIIIa inhibitors block fibrinogen/fibrin attachment to GPIIbIIIa, thus preventing platelet-platelet cross-linking and GPIIbIIIa-mediated platelet activation *via* phospholipase C: examples include Abciximab™ (Gabriel & Oliveira 2006), Eptifibatide™ (Zeymer & Wienbergen 2007), and Tirofiban™ (Bukow *et al.*, 2006).

Platelet aggregation inhibitors are a large family of platelet inhibitors on their own; they act on aggregation-associated platelet integrins PAR1/PAR4, P2Y₁/P2Y₁₂, TP, and their associated binding targets. For example, the popular Aspirin™ (Watson & Chee YL, 2008; Yasuda *et al.*, 2008) blocks thromboxane A₂ generation (which triggers TP activation), and Prasugrel™ (Niitsu *et al.*, 2005) inhibits ADP receptors P2Y₁/P2Y₁₂ to prevent amplification of platelet activation. Plasminogen activators such as streptokinase convert plasma derived plasminogen into plasmin, which is an enzyme that breaks down fibrin fibrils, and represent the so-called clot-busting drugs rather than clot preventing drugs (Juttler *et al.*, 2006). Direct thrombin inhibitors such as Argatroban™ (Bauer, 2006) are almost self-explanatory, they inhibit thrombin and hence thrombin generation of fibrin, which drastically reduces platelet-platelet cross-linking. Lastly, there are non-specific chemical compounds such as citrate, EDTA, and oxalates, which chelate plasma Ca²⁺ (Chappell, 2007) and in turn reduce Ca²⁺ influx into platelets thus inducing platelet activation; these compounds are not used *in vivo* due to their non-specific nature.

Antithrombotics are primarily employed in clinical scenarios where thrombus formation could lead to life-threatening ischemic events such as stroke or pulmonary embolism (Agnelli & Sonaglia, 2002; Katira *et al.*, 2005). Hence antithrombotics are widely used during and post surgery and their popularity is expected to rise with the increase in the prevalence of cardiovascular disease. However, it should be noted that many current drugs (warfarin, heparin, and their analogues) are mostly focused on the coagulation cascade and not necessarily on the platelets themselves. This could be problematic as platelets will still attach to the damaged endothelium and cross-link through fibrinogen even in the absence of thrombin and clotting factors; platelet-rich

thrombi could still be formed under these conditions and could cause life threatening events. For example, heparin induced thrombocytopenia (HIT) is a disease resulting from the use of heparin that may lead to life-threatening thrombotic events (Castelli *et al.*, 2007; Joost *et al.*, 2008; Linkins & Warkentin 2008). Hence understanding the function of platelet integrins and their associated signalling mechanisms may help identify therapeutic targets for the generation of future antithrombotics (Vanhoorelbeke *et al.*, 2003; Clementson & Clementson 2008). In particular, the GPIb-IX-V receptor and its interaction with vWf were mentioned previously as being upstream of most platelet activation mechanisms and are a useful avenue to explore for potential therapeutics (Clementson & Clementson, 2008). In this study, I will verify the anti-thrombotic activity of RGD and, more importantly, investigate the efficacy of a peptidomimetic inhibitor of the GPIb-vWf interaction.

1.4 Peptidomimetics

Peptidomimetics are short amino acid sequences that have shape and hydrophobic profiles that provide epitopic behaviour. Based on their attributes, they can be screened selectively for ligand- or receptor-like activity to target specific binding sites. The prospect of deploying such polypeptides in a therapeutic setting presents a promising lead in rational drug-design. Novel peptidomimetics can be derived from peptide arrays of random amino acid sequences, or overlapping sequences from a ligand or receptor (Grainger *et al.*, 2007). In either case, the sequences with binding potential and possible inhibitory activity are probed with a target protein that may or may not bind sequences from the array. The materials that bind to the array can in turn be detected by a variety of detection systems, often based on antibodies in a manner similar to a western blot.

Positive sequences from peptide arrays may be tested for binding activity in two ways: by laboratory testing of compound libraries (Wiley & Rich, 1993), or by the application of bioinformatic models (Del Carpio Munoz *et al.*, 2006; Urbanj *et al.*, 2006). One approach involves manufacturing all the candidate peptides and threading them through functional assays, and the other, perhaps more cost-effective method, involves computational interpolations of the free-energy release associated with peptide binding to the active sites of target proteins (Del Carpio Munoz *et al.*, 1999; Yoshimori *et al.*, 2001).

Applications of peptidomimetics are numerous; for example, a peptidomimetic was used to induce apoptosis of malignant leukemic cells without affecting healthy tissue Walensky *et al.* (Walensky *et al.*, 2004); peptidomimetics have been used to inhibit thrombin (Hauptmann, 2002). Pertinent to this study, one of the best-known peptidomimetics, RGD was coupled to liposomes and used to target activated platelets as a method of vascular drug delivery (Gupta *et al.*, 2005). The RGD peptide sequence is a motif found in fibronectin, vitronectin, osteopontin, collagens, thrombospondin, and fibrinogen, and can mediate integrin adhesion and cellular communication (Rouslahti & Pierschbacher, 1987). The RGD motif disrupts platelet aggregation by binding to the platelet glycoprotein IIb/IIIa integrin receptor (GPIIbIIIa) to cause competitive exclusion of fibrinogen from its binding site (Beer *et al.*, 1992). RGD and RGD-containing conjugates are effective antithrombotics (Gould, 1994) because fibrinogen-mediated bridging and platelet aggregation are essential steps in primary haemostasis. The GPIIbIIIa - fibrinogen interaction is clinically relevant and a new generation of antithrombotics specifically targets this interaction (Gabriel & Oliveira, 2006). To this end, a number of laboratories have defined the pharmacophore of RGD (Ojima *et al.*,

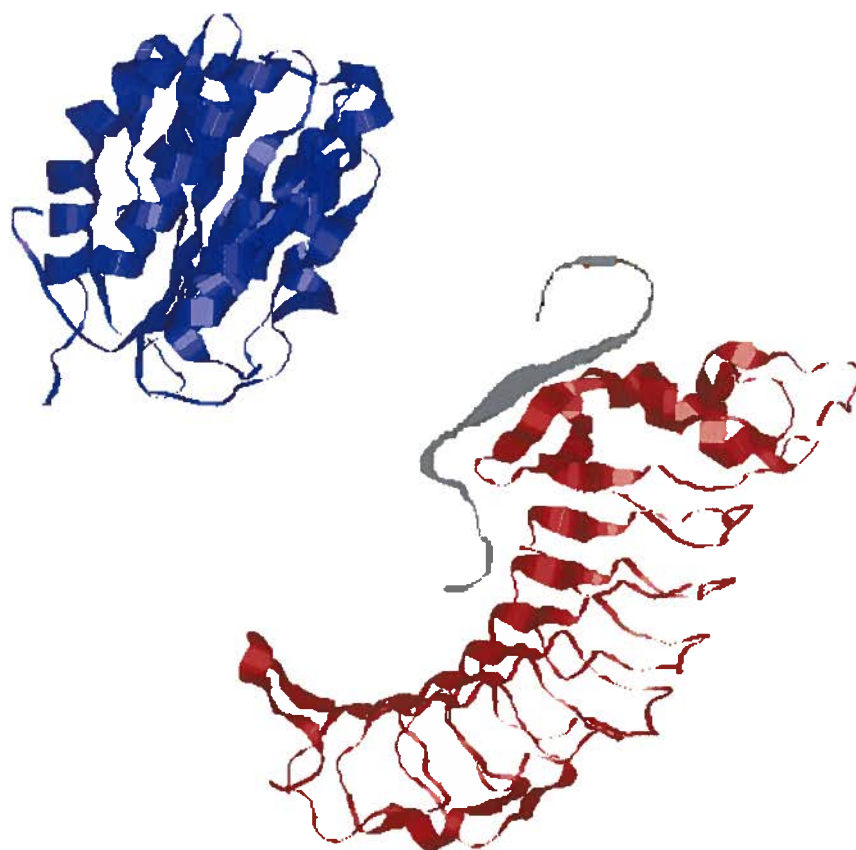


Figure 1.41. MIAX Interpolated vWf Peptidomimetic (SHAYIGLKDR) Inhibition of GPIb-vWf interaction. The bottom protein domain in red is a truncated vWf-binding active site of GPIb. The top protein in blue is von Willebrand factor. The peptide in grey binds GPIb at its vWf-binding active site, and prevents vWf attachment to GPIb.

1995), and explored a wide variety of chemical modifications on simple peptidomimetic structures designed to compete with fibrinogen, in order to improve either their binding affinity for GPIIb/IIIa or their pharmacokinetic profile (Walensky *et al.*, 2004; Gould, 1994; Gabriel & Oliveira, 2006; Ojima *et al.*, 1995; Lee & Marchant, 2003; Mousa *et al.*, 2001). RGD, RGD variants, and RGD mimics have proven to be successful antithrombotics both *in vitro* and *in vivo* (Nicholson *et al.*, 1991; Sheu & Huang, 1994). Although RGD seems somewhat promising, it interferes with GPIIb/IIIa's interaction with fibrinogen, which is a step of platelet activation that occurs late in the activation cascade, especially compared to the vWf's interaction with the GPIb-IX-V complex and its consequent effects.

Relying on RGD-based antithrombotics still leaves activated and degranulated platelets. Since platelet granules are not renewed (Harrison & Cramer 1993), patients receiving RGD-based drugs would inevitably lose those activated platelets to macrophages, thereby lowering their platelet count. Hence, it is more beneficial to look for upstream targets in the platelet activation cascade that prevent platelets from becoming activated in the first place. The interaction of vWf with the GPIb-IX-V complex is an excellent upstream target for drug interference. For this purpose, we had identified SHAYIGLKDR as a high affinity peptide binding the platelet glycoprotein GPIb. This peptide was derived by synthesizing overlapping peptides from the native sequence of vWf on an L-peptide array and identifying active peptides by binding to GPIb. Using the MIAx bioinformatics program (Del Carpio Munoz *et al.*, 1999; Yoshimori *et al.*, 2001; Del Carpio Munoz *et al.*, 2003) SHAYIGLKDR was mapped to the A1 domain of the vWf sequence and was projected by MIAx to bind GPIb in the

GPIIb-vWf interactive domain. It was hoped that by locating to the GPIIb interactive surface, this peptide would inhibit vWf binding to the same location.

1.5 Macromolecular Carriers and Conjugation

In order to be clinically useful, a mimetic compound must evade rapid elimination from the host and demonstrate high efficacy at comparatively low doses. RGD, RGD variants, and RGD mimics suffer from limited *in vivo* retention due to their small size. A well known solution to this problem is to couple such peptides to long-circulating materials. Studies have described the conjugation of RGD to albumins (Temming *et al.*, 2006), to polyethylenimine – polyethylene glycol (Kim *et al.*, 2003) and to liposomes (Janessa *et al.*, 2003). Other macromolecules, such as hyperbranched polyglycerols are also potentially viable choices as carriers. HPGs are water soluble, biocompatible polyether polyols (Sunder *et al.*, 2000; Sunder *et al.*, 2000) that can be synthesized in a controlled manner with predetermined molecular weights and narrow molecular weight distributions (Kainthain *et al.*, 2006). There are two general choices when selecting a macromolecular carrier: monovalent/bivalent carriers, and polyvalent dendrimers (Figure 1.51). The first encompasses carriers such as linear PEG molecules to which peptides may be attached at one or both ends; the latter includes carriers with many “dendrites” that consequently can host a high number of peptides. While both serve to increase the MW of the peptide they carry, the latter carriers have the potential of also altering the equilibrium dynamics by presenting their target as a higher local concentration of peptides. Thus macromolecules with dendrites were chosen as the carriers for this study.

Recently Kainthan *et al.* reported the synthesis of very high molecular weight HPGs (MW values up to 1.48×10^6) with low PDI: where $PDI = M_w/M_n = 1.1-1.4$ where

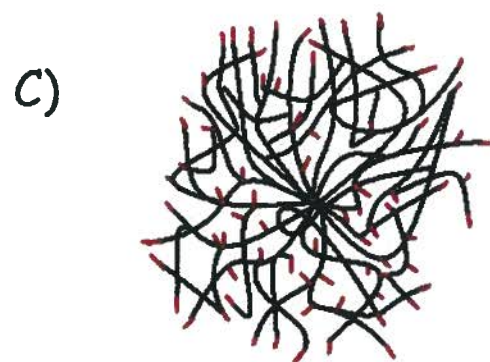


Figure 1.51. Carrier Valency. Diagrammatic representation of (A) monovalent, (B) bivalent, and (C) polyvalent carriers. Red ends on panel A, B, and C denote peptides.

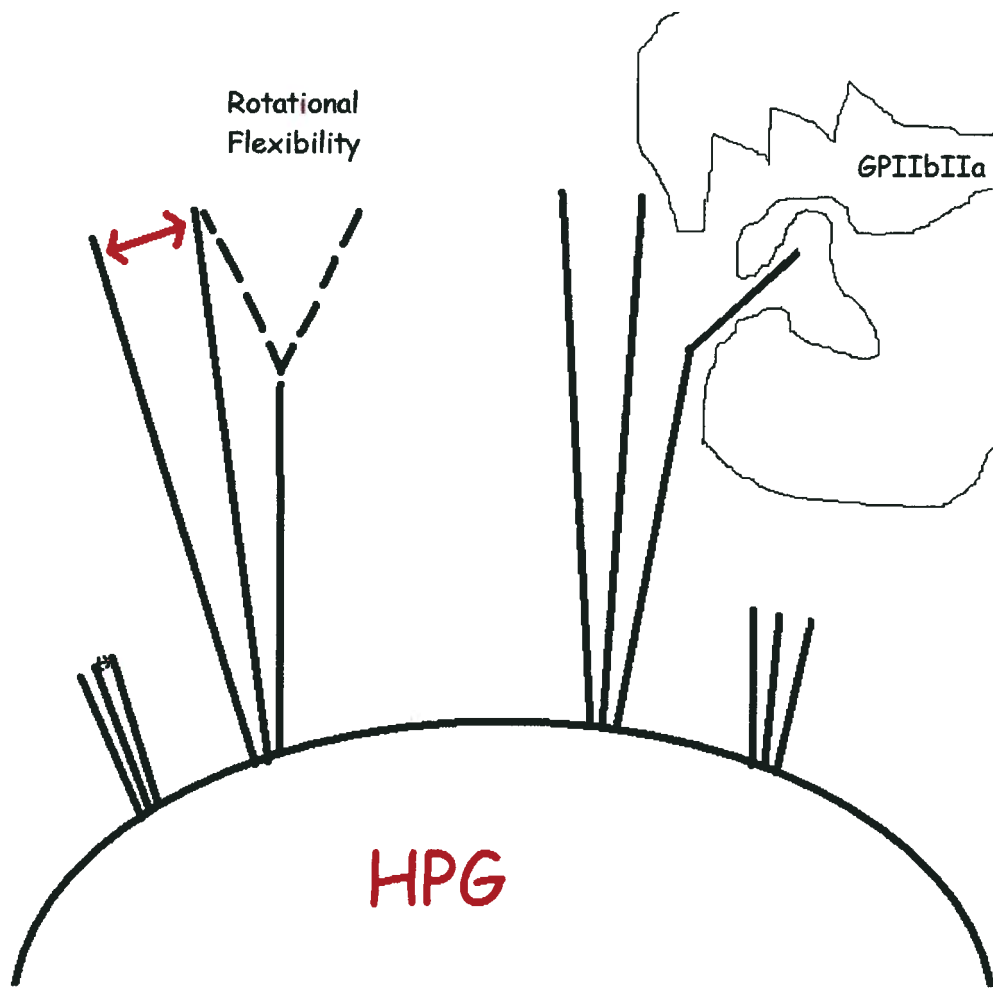


Figure 1.52. Relationship Between Linker Length and Degrees of Freedom in High Density Brushes. The HPG (10 nm) is not to scale relative to the length of the peptides (2 nm). The left side of the figure shows the differences in the available space (red double tipped arrows) for the tips of the peptides conjugated to HPG at different heights. The right side of the figure demonstrates that some level of flexibility may be required for binding to receptors (GPIIbIIIa).

M_w and M_n are the weight and number molecular weights respectively (Kainthain *et al.*, 2006). These polymers show excellent biocompatibility properties both *in vitro* (Kainthan *et al.*, 2007) and *in vivo* (Kainthan & Brooks. 2007). The plasma circulation half lives were found to depend on the molecular weight and half lives as high as 60 hours were achieved for high molecular weight polymers (Kainthan & Brooks, 2007). As the number of hydroxyl groups approximately equals the degree of polymerization, synthesis of higher molecular weight HPGs is a major development given the difficulty of synthesizing high molecular weight dendrimers. These materials have numerous applications in nano-medicine and one such application is the use of HPGs as carriers of peptides for biomedical applications where multivalency/polyvalency can be exploited.

The hydroxyl groups on HPG can be coupled to sulfhydryl groups on cysteines in a peptide through divinyl sulfone (DVS). First the HPG is functionalized by coupling to DVS, the resulting HPG molecule with DVS (HPG-VS) acquires an acryl group that is thiol-selective, which is excellent for coupling to the sulfhydryl group on a cysteine (Bulmus *et al.*, 2000). A terminal cysteine residue can be added to the peptidomimetic sequence for this purpose. In addition, a poly-glycine linker is used as a spacer, which could grant the peptidomimetic more flexibility as well as more space to maneuver (Figure 1.52). Due to the novelty of high molecular weight HPG, no information was available about its potential to function as a carrier for peptidomimetics. To test the potential of this molecule as a carrier for peptidomimetics, the well-known peptidomimetic, RGD was tested instead of directly proceeding to our novel peptide, SHAYIGLKDR. Therefore, our theories of polyvalency were tested initially with the

RGD molecule and then the optimized parameters from the RGD study were applied to the novel peptide.

1.6 Peptide Polarity and Chirality

Conjugation of peptides to a surface such as a macromolecular carrier automatically confers polarity to that peptide. This directionality may, or may not affect the peptide's activity by keeping the pharmacophore at a distance from the target site and closer to the surface of the macromolecular carrier; or by orienting it in a way that would prevent the peptide from fitting to its target. Hence it is always prudent to consider both forward and reverse (reverso-) forms of a peptide during conjugation (Figure 1.61). Short peptides sequences such as RGD are less susceptible to this problem compared to longer peptides such as SHAYIGLKDR, especially when the actual pharmacophore is not known in detail.

In addition to the directional orientation imparted by conjugation to a carrier, peptide specificity is also controlled by charge and side-chain orientation. Although these two factors are often considered hand-in-hand, charge interactions are generally less specific than side-chain interactions, as side-chain orientation is important for fitting the peptide into a specific binding pocket that exists in a relatively fixed orientation. However, it is prudent to evaluate which of these factors dominates experimentally because these principles are general but may not be applicable to selected situations. Hence, for this study we also created the peptidomimetics as D-enantiomers (Figure 1.62), those peptides with opposite backbone/side-chain orientations, as well as their D-reverso counterparts. This design was intended to evaluate whether the specificity of the SHAYIGLKDR peptide is primarily charge driven or orientation driven. Hence, the D-

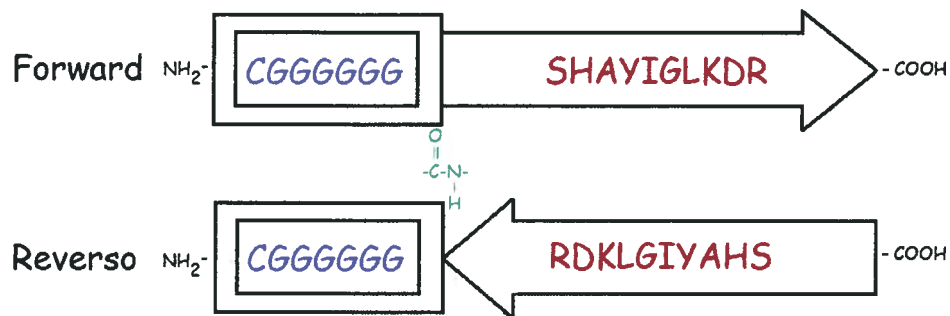


Figure 1.61. Nomenclature of Peptide Polarity. All amino acids represented by their single letter amino acid names are written from the amino terminus to the carboxy terminus (left to right). The linker peptide is denoted in blue, and the peptidomimetic peptide is shown in red as either “forward” or “reverse.” This convention applies to the amino sequence only; a normal peptide bond (in green) indicates that the amino- and carboxy- termini were not altered/reversed. Large arrows housing the peptide sequences indicate arbitrary labelling convention for “forward” and “reverse.”

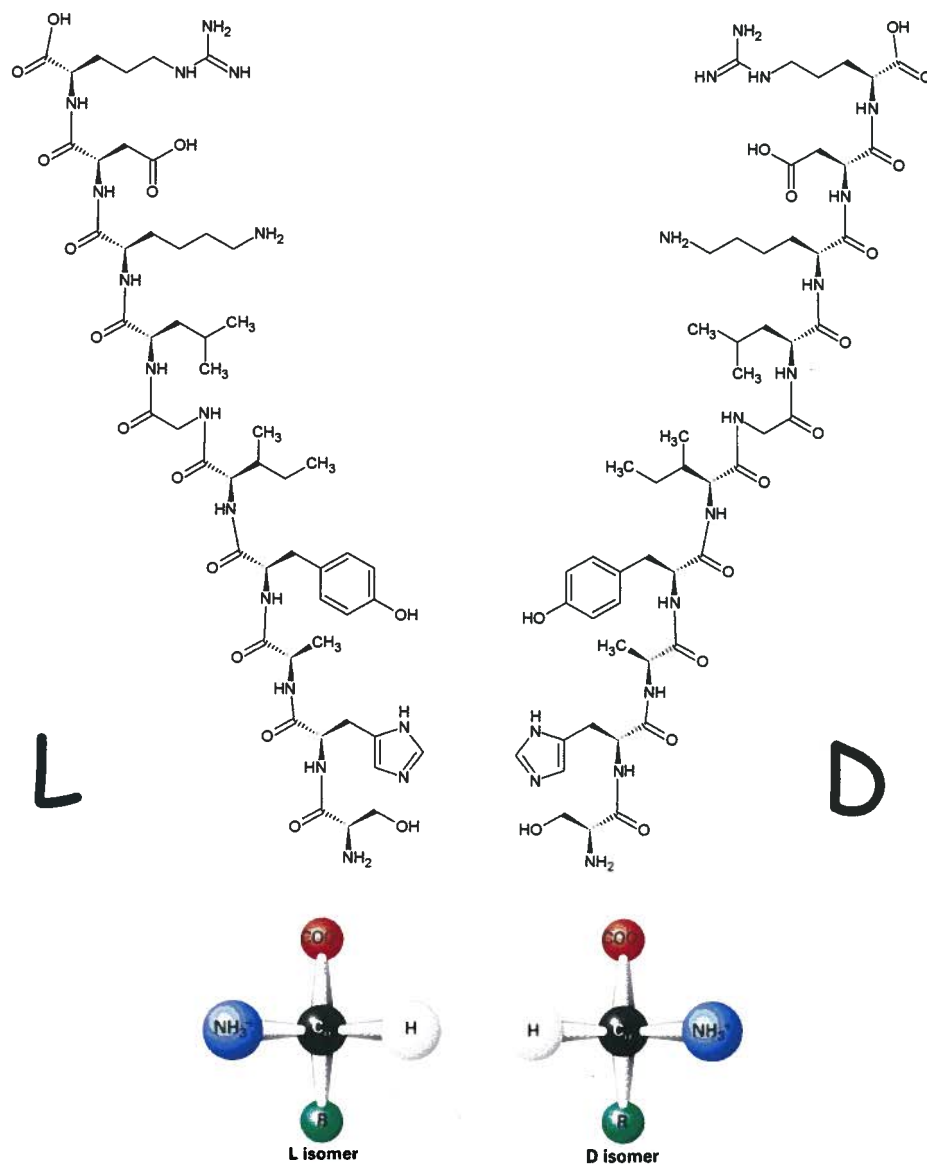


Figure 1.62. The SHAYIGLKDR Peptide and its D-enantiomer. The SHAYIGLKDR peptide is represented as both L- and D- enantiomers, which are mirror images of one another. Coloured models at the bottom of the figure are guides to the L & D naming convention for amino acids.

enantiomers serve as an important control for SHAYIGLKDR as the peptide was originally derived as an L-enantiomer. As well, ideally for drug design, a peptide that resists *in vivo* enzymic degradation would be an asset and this was a further rationale for the assessment of D-enantiomer function.

1.7 Hypothesis

We hypothesize that it is possible to create a new class of antithrombotic materials based on the combination of a peptidomimetic and a macromolecular carrier such that the peptidomimetic's anti-platelet potential is enhanced by conjugation. Hence, we also hypothesize that:

- 1) As RGD is an inhibitor of the platelet-fibrinogen interaction, L-SHAYIGLKDR is an inhibitor of the platelet-vWf interaction.
- 2) RGD and SHAYIGLKDR do not trigger spontaneous platelet activation by degranulation/CD62 surface expression, fibrinogen binding, vWf binding, and/or GPIIbIIIa activation.
- 3) HPG of molecular weights 3 kDa, 100k Da, and/or 500 kDa do not trigger spontaneous platelet activation by degranulation/CD62 surface expression, fibrinogen binding, vWf binding, and/or GPIIbIIIa activation.
- 4) HPG of molecular weights 3 kDa, 100k Da, and/or 500 kDa do not inhibit platelet-fibrinogen and/or platelet-vWf interaction.
- 5) Conjugates resulting from combinations of HPG and RGD do not trigger spontaneous platelet activation by degranulation/CD62 surface expression, fibrinogen binding, vWf binding, and/or GPIIbIIIa activation.

- 6) Conjugates resulting from combinations of HPG and RGD are inhibitors of platelet-fibrinogen interactions: that is, the activity of RGD is conserved after conjugation.
- 7) The resulting activity of HPG-RGD conjugates is solely dependent and specific to the RGD moiety.
- 8) Conjugates resulting from combinations of HPG and SHAYIGLKDR do not trigger spontaneous platelet activation by degranulation/CD62 surface expression, fibrinogen binding, vWf binding, and/or GPIIbIIIa activation.
- 9) Conjugates resulting from combinations of HPG and SHAYIGLKDR are inhibitors of platelet-vWf interactions: that is, the activity of SHAYIGLKDR is conserved after conjugation.
- 10) The amplification of activity of either RGD or SHAYIGLKDR peptide would be dependent on the size of HPG and/or the amount of peptide conjugated per HPG molecule.
- 11) The resulting activity of HPG-SHAYIGLKDR is solely dependent upon and specific to the SHAYIGLKDR moiety.
- 12) Forward and reverse versions of the SHAYIGLKDR peptide would have different activities after conjugation to HPG as a result of polarity considerations.
- 13) L- and D- enantiomers of SHAYIGLKDR peptide have different activities in the inhibition of the interaction between GPIIb and vWf.

Chapter 2 – Methods

2.1 Peptides and Proteins

The peptidomimetic RGDF was selected for its high I_{C50} , and a 6-mer cysteine-polyglycine linker was added to create CGGGGGGRGDF, (MW = 882) and was synthesized by the University of BC's Nucleic Acid and Peptide Synthesis unit to >90% purity as tested by HPLC.

A 7-mer poly-glycine linker sequence was defined such that with the active peptide SHAYIGLKDR the peptidomimetic sequences (MW = 1605) became: L-CGGGGGGSHAYIGLKDR (L-peptide), L-CGGGGGGGRDKLGIYAHS (L-reverso peptide), D-CGGGGGGSHAYIGLKDR (D-peptide), D-CGGGGGGGRDKLGIYAHS (D-reverso peptide). These were synthesized by the University of BC's Nucleic Acid and Peptide Synthesis unit at the Brain Research Centre to >93% purity as tested by HPLC.

The peptides are dissolved in HEPES buffered saline (HBS, 10 mM HEPES, 150 mM NaCl, pH 7.40) for spectroscopic studies and *in vitro* assays.

2.2 Preparation of Human Platelets

As approved by CBS' and UBC Ethics Board, samples of whole blood were drawn from healthy, consenting donors into 2.7 - 4.0 mL citrate tubes (BD Biosciences, USA). Platelet rich plasma (PRP) was prepared from whole blood by centrifugation in a Beckman (CS-6R) bench-top centrifuge ($r = 203.57\text{mm}$, Beckman Coulter, USA) $164\times g$ for 15 minutes. PRP from a number of unrelated donors was evaluated on an Adiva 120 Hematology Analyzer (Bayer, Canada) and standardized to a concentration of 300×10^9 platelets/L in HEPES buffered saline (HBS, 10 mM HEPES, 150 mM NaCl, pH 7.4).

2.3 HPG-RGD Conjugates

2.31 Polyglycerols and Conjugation

Hyperbranched polyglycerols of molecular weights of 3 kDa, 100kDa, and 515 kDa were synthesized as described previously (Kainthan *et al.*, 2006). The conjugation of the peptide to the HPG was achieved through the sulfhydryl group of cysteine coupling to vinyl sulfone functionalized polymers. A typical reaction procedure (HPG-RGD conjugate C-7) was as follows. Initially, the HPG-515 kDa polymer (100 mg) was dissolved in 3 mL dimethyl sulfoxide (DMSO) and up to 20% of the $n \sim 7000$ theoretical hydroxyl groups were deprotonated with 20 mg potassium hydride (30 wt % dispersion in mineral oil, Sigma-Aldrich, Canada). Subsequently, 20 μ L of divinyl sulfone (corresponding to a polymer-peptide ratio of 1:1000) was added and stirred at 22 °C for 12 hours. After the reaction, methanol was added and the reaction mixture was passed through an Amberlite IRC-150 cation exchange column (Sigma-Aldrich, Canada) to remove the potassium ions. The polymer was then precipitated in acetone and dried. For the peptide coupling, 5 mg vinyl sulfone functionalized polymer was dissolved in 2 mL DMSO (Sigma-Aldrich, Canada) and stirred with an excess amount of peptide (15 mg) for 2 days at 22 °C. The excess peptide was removed by dialysis (cellulose acetate membrane, MW cut-off 1000, Spectrum Laboratories Inc., USA) against HEPES buffered saline and the conjugate was collected by lyophilization (Figure 2.31). The other conjugates were synthesized using appropriate amounts (Table 3.11) of divinyl sulfone and peptide.

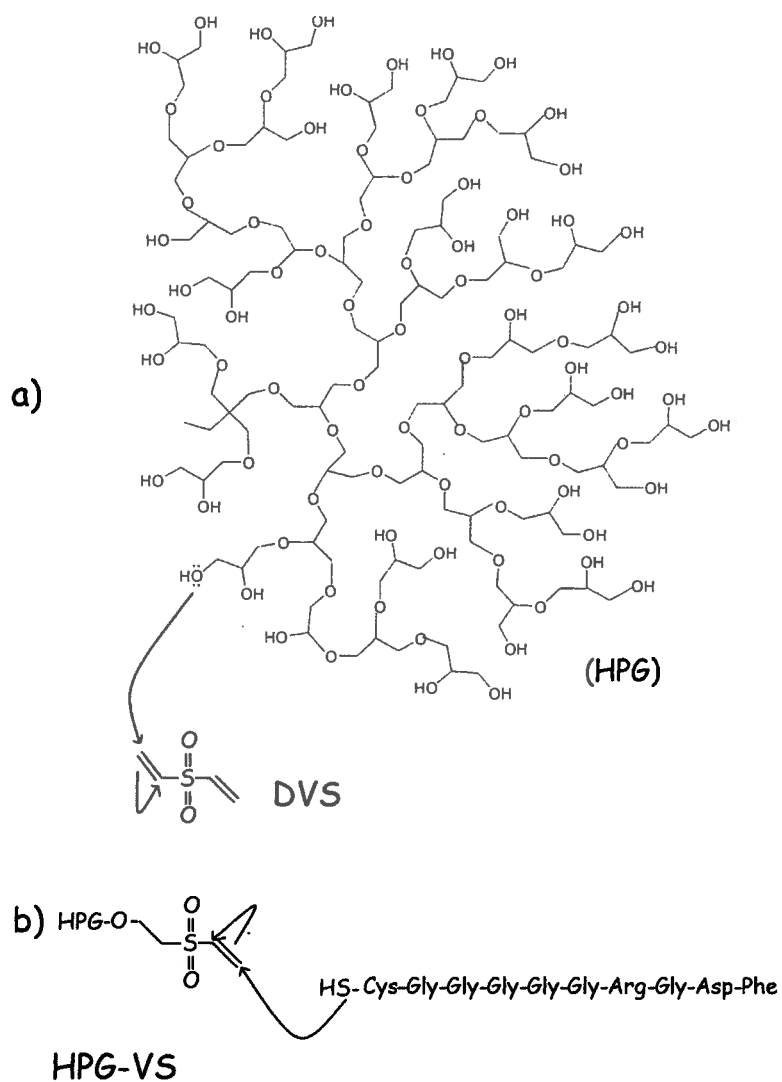


Figure 2.31. Functionalization of HPG and Conjugation of RGD Peptides.

a) functionalization of HPG hydroxyl groups with divinyl sulfone (DVS); b) conjugation of peptides to functionalized HPG *via* cysteine side chain.

2.32 Characterization of the HPG-RGD Conjugates

The HPG-RGD conjugates were characterized for peptide substitution levels by UV absorption at 260 nm ($\epsilon = 144 \text{ cm}^{-1}\text{M}^{-1}$) on an ND-1000 Spectrophotometer, (Nanodrop Technologies, USA). A calibration curve was made using standards made from the free peptide molecules at a range of concentrations ($1.0 \times 10^{-7} \text{ M}$ to $6.0 \times 10^{-3} \text{ M}$).

2.33 Flow Cytometry

Effects of the Native HPG on Resting and Activated Platelets

First we examined the effect of the various molecular weights of unconjugated HPG on resting and activated platelets. For resting platelets, 45 μL aliquots of HBS were mixed with 5 μL PRP and 5 μL of 3 kDa, 100 kDa, and 500 kDa HPG polymers at each of $1.0 \times 10^{-3} \text{ M}$, $1.3 \times 10^{-7} \text{ M}$, and $2.9 \times 10^{-8} \text{ M}$ concentrations and incubated for 40 minutes, then 5 μL of human fibrinogen (Sigma-Aldrich, Canada), at 5 mg/mL dissolved in bicarbonate buffer (100 mM NaHCO_3 , pH 8.30) was added and the incubation continued for 30 min before the addition of 5 μL 1.5 mg/mL FITC-conjugated monoclonal mouse anti-human fibrinogen IgG (Biocytex, France) and continued incubation in the dark for 30 min. Similarly, to assay the effect of unconjugated HPG on activated platelets, 5 μL 10 mM MnCl_2 to activate GPIIb/IIIa (Walsh *et al.*, 2004) was included in the above assay.

Effects of the Conjugated HPG on Resting Platelets

Thereafter, I determined whether the conjugated HPGs were capable of activating resting platelets. For this, the fibrinogen-anti-fibrinogen detection system of the above

assay was replaced by 5 μ L 2 mg/mL of PE-conjugated mouse anti-human CD62 IgG1 (Beckman-Coulter, Canada) to detect P-selectin expression on the platelet surface.

Effects of the Conjugated HPG on Activated Platelets

Finally, I examined the effect of the RGD-conjugated HPGs first on the resting platelets' ability to bind fibrinogen, then on activated platelets using appropriate modifications of the above assay systems. Negative controls included incubating with mouse IgG-FITC of the same isotype, and/or omitting the conjugate, and/or omitting the addition of $MnCl_2$ to activate platelet GPIIb/IIIa which allows for the detection of baseline binding to fibrinogen. Positive controls for platelet fibrinogen binding did not contain conjugates. After the incubations, the samples were diluted and fixed with 0.2% formalsaline (0.2% formaldehyde, 150 mM NaCl, pH 7.20) before being submitted for analysis on the FACS Canto II flow cytometer (BD Biosciences, USA).

Enzyme Cleavage

RGD conjugated to the 3 kDa HPG was dissolved in HBS to a final concentration of 1 mM and treated with 1 mM trypsin-TPCK (Sigma-Aldrich, Canada) for 15 minutes at 37 °C. Enzyme cleavage was stopped with the addition 2 mM soybean trypsin-inhibitor (SBTI, Sigma-Aldrich, Canada) for another 15 minutes. Controls included pre-mixed and incubated trypsin-TPCK with SBTI added to platelets only, to peptides only, and to the RGD conjugated HPG. Enzyme treatment was followed by flow cytometry as already described.

2.34 Microscopy

In a standard ELISA plate, PRP was incubated at 37°C for 100 minutes with 10 μ L 100 mM MnCl_2 , and an amount of conjugate with a final conjugate concentration equal to the conjugate's $\text{I}_{\text{C}50}$ and a final platelet concentration of 300×10^9 cells/L in a 200 μ L volume. Negative controls consisted of platelets incubated alone, while positive controls included 10 μ L 100 mM MnCl_2 as a platelet agonist. These samples were examined at 400 \times magnification on a Leica DMIL inverted microscope (Leica Microsystems, Germany) with 1-S55 filter. Pictures were taken with Micropublisher 3.3 Cooled RTV and the QCapture program (Q-Imaging, Canada).

2.35 Aggregometry

PRP (300×10^9 cells/L, final concentration) was incubated at 37°C for 100 minutes with conjugates or unsubstituted HPG at a final concentration equal to the $\text{I}_{\text{C}50}$ of that conjugate, in a total volume of 315 μ L. The samples were loaded into the aggregometer (Chrono-Log, USA) and compared to a platelet poor plasma derived from the same blood source, produced by high speed centrifugation. To initiate aggregation 25 μ L of 100 mM MnCl_2 was added and the aggregation curve was recorded for 12 minutes.

2.4 HPG-SHAYIGLKDR Conjugates

2.41 Polyglycerols and Conjugation

Synthesis and conjugation of 500 kDa hyperbranched polyglycerols were conducted as described previously. (Kainthan, Zhang) In a typical reaction procedure, the HPG-500 kDa polymer (100 mg) was dissolved in 3.0 mL dimethyl sulfoxide (DMSO, Sigma-Aldrich, Canada) and up to 20 % of the $n \sim 7000$ theoretical hydroxyl groups were

deprotonated with 20 mg potassium hydride (30 wt % dispersion in mineral oil, Sigma-Aldrich, Canada). Divinyl sulfone, 2 μ L, (DVS, corresponding to a polymer-peptide ratio of 1:100) was added and stirred at 22 °C for 12 hours. After the reaction, 2.0 mL 5.0 M HCl was added to quench the remaining KH and the reaction mixture was adjusted to neutral pH, then dialyzed through a 1000 kDa MW cut-off membrane (Spectrum Laboratories Inc., USA) to remove the potassium ions, and the VS-HPG (HPG-vinyl sulfone, bifunctionality of DVS reduced to VS after attachment to HPG, Figure 2.41) was recovered by lyophilization. For peptide coupling, 5 mg vinyl sulfone functionalized polymer was dissolved in 2 mL DMSO and stirred with an excess amount of peptide (6 mg) for 4 days at 22 °C. Excess peptide was removed by dialysis through a 3000 kDa MW membrane, (Spectrum Laboratories Inc., USA) against deionized water and the conjugate was collected by lyophilization (Figure 2.41). All the conjugates were synthesized using similar amounts of divinyl sulfone and peptide. The conjugates are identified with abbreviated names: L₁₀ through DR₁₀₀ (Table 3.21), with the first letter denoting the chirality of the peptide, the second letter (if any,) denoting the polarity, and the subscript denoting the conjugation ratio of peptides to HPG. For example, LR₁₀ represents an HPG conjugate with 10 L-Reverso peptides per HPG molecule.

2.42 Characterization of the VS-HPG Constructs

The initial substituted VS-HPG were dissolved in DMSO and their substitution levels were quantified using a standard thiol-estimation assay (Grasetti *et al.*, 1967; Reiner *et al.*, 2002) by reaction with excess 2-mercaptoethanol for 2 hours and then titration of the excess 2-mercaptoethanol with 4,4-dithiodipyridine (DTDP). The molar

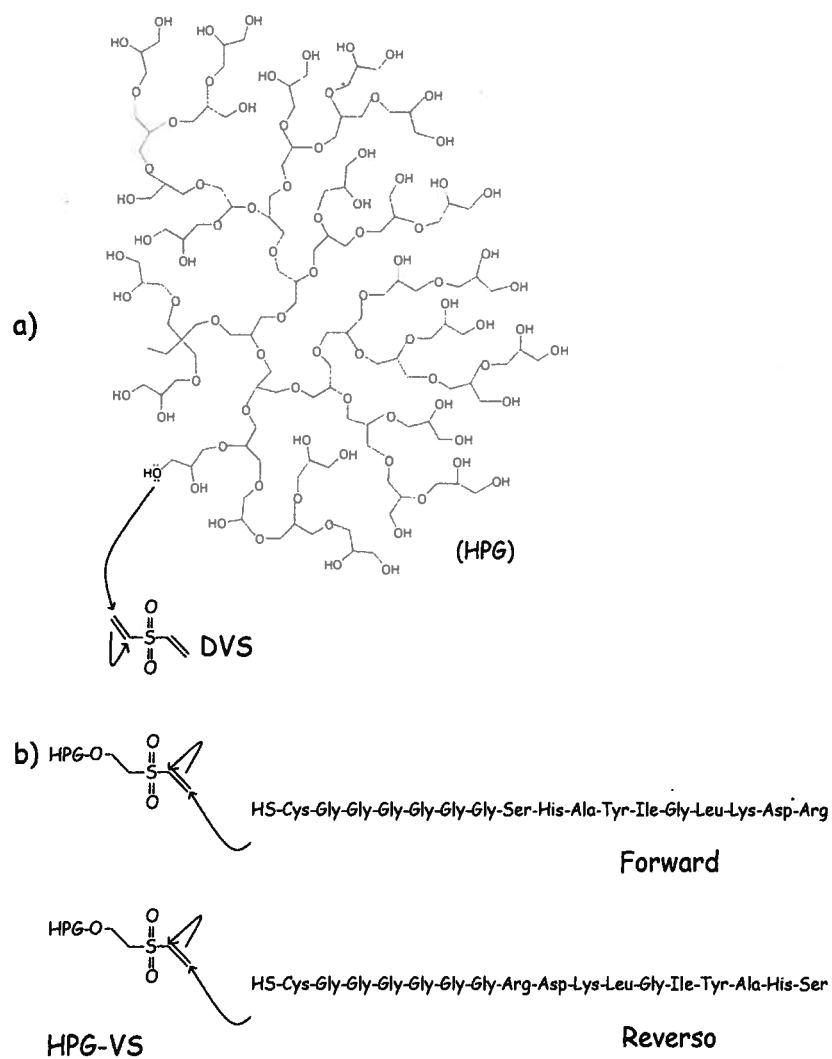


Figure 2.41. Functionalization of HPG and Conjugation of SHAYIGLKDR

Peptides. a) functionalization of HPG hydroxyl groups with divinyl sulfone resulting in HPG-VS; b) conjugation of peptides to functionalized HPG *via* cysteine side chains.

absorption of the resulting 4-thiopyridone was measured at A_{324} nm ($\epsilon = 19,800 \text{ M}^{-1} \text{ cm}^{-1}$) with a spectrophotometer (Farooqi *et al.*, 1984).

2.43 Characterization of the HPG-peptide Conjugates

The HPG-peptide conjugates were assessed for substitution level by UV absorption at 278 nm ($\epsilon = 1440 \text{ cm}^{-1} \text{ M}^{-1}$) on an ND-1000 Spectrophotometer, (Nanodrop Technologies, USA). A calibration curve was made using standards made from the free peptide molecules at a range of concentrations ($1.0 \times 10^{-7} \text{ M}$ to $1.2 \times 10^{-3} \text{ M}$).

2.44 Flow Cytometry

Effects of the Native and Peptide-conjugated HPG on Resting Platelets

First I examined the effect of the native and peptide-conjugated HPG on resting platelets. In a flow cytometer tube, 40 μL aliquots of HBS were mixed with 5 μL PRP and 5 μL of the material to be tested: 500 kDa HPG; peptidomimetic peptides; or peptide-conjugated HPG at $1.0 \times 10^{-3} \text{ M}$ to $1.0 \times 10^{-9} \text{ M}$. After 40 minutes of incubation at ambient temperature, 5 μL 0.01 mg/mL FITC-conjugated polyclonal sheep anti-human vWf IgG (Abcam, USA) or 5 μL of 2 mg/mL PE-conjugated monoclonal mouse anti-human CD62 IgG (Beckman-Coulter, Canada) was added and incubation was continued in the dark for 30 min. Thereafter the samples were diluted and fixed with 1.0 mL 0.2 % formalsaline (0.2% formaldehyde, 150 mM NaCl, pH 7.20) before analysis on a FACS Canto II flow cytometer (BD, USA).

Effects of the Native and Peptide-conjugated HPG on Activated Platelets

Finally, we examined the effect of native HPG, peptidomimetic peptides, and peptide-conjugated HPG on activated platelets using modifications of the above assay

systems. Platelets were either activated with 5 μ L 4.2 mg/mL ristocetin (Chrono-Log, USA) or 100U thrombin (T6884, Sigma-Aldrich, Canada) with 5 μ L GPRP fibrin inhibitor (G5779, Sigma-Aldrich, Canada) dissolved in HBS to determine whether peptides and peptide-conjugates can mitigate vWf and thrombin mediated platelet activation. Controls included incubation with mouse IgG-FITC / IgG-PE (Beckman-Coulter, Canada) of the same isotype, and/or omitting the conjugate.

Enzyme Cleavage

The LR-peptide and conjugate LR₁₀₀ were dissolved in HBS to a final concentration of 0.1 mM and treated with 2 mg/mL Trypsin-TPCK (Sigma-Aldrich, Canada) for 4 hours at 37 °C. Enzyme cleavage was stopped with the addition 5 mg/mL soybean trypsin inhibitor (SBTI, Sigma-Aldrich, Canada) for another 30 minutes. Controls included pre-mixed and incubated trypsin with SBTI added to platelets only, to peptides only, and to the peptide conjugated HPG. Enzyme treatment was followed by flow cytometry as already described.

GPIb Signaling Through GPIIb/IIIa Activation

Signal transduction through GPIb will eventually cause conformational changes of GPIIb/IIIa resulting in its conversion to its active form which allows fibrinogen/fibrin binding (Figure 1.21), as detected by a FITC conjugated anti-PAC-1 antibody. Anti-PAC-1 antibody detects only the active/open form of GPIIb/IIIa. 35 μ L resting platelets were incubated with 5 μ L L-peptide and L₁₀₀ conjugate at their respective I_{C50} concentrations for 1 hour before activation via 5 μ L 4.2 mg/mL ristocetin and addition of 5 μ L monoclonal FITC conjugated anti-PAC-1 antibody (BD Biosciences, USA). Negative

controls included incubation of resting platelets with mouse IgM-FITC (1/10 dilution in HEPES buffer, BD Biosciences, USA) of the same isotype, resting platelets with 5 μ L anti-PAC-1 FITC antibody, and resting platelets incubated with L-pep and L₁₀₀ conjugate without treatment by ristocetin; the positive control involves activation with 5 μ L 4.2 mg/mL ristocetin and incubation with 5 μ L anti-PAC-1 FITC antibody.

2.45 Microscopy

In a standard ELISA plate, wells received samples corresponding to the same composition of fluids as the flow cytometry assays performed to determine the effect of conjugated HPG on activated and resting platelets. In the ELISA plates, the reactions were fixed with 150 μ L of formolsaline. The samples were examined at 400 \times magnification on a Leica DMIL inverted microscope (Leica Microsystems, Germany) with a 1-S55 filter. Pictures were taken with Micropublisher 3.3 Cooled RTV and the QCapture program (Q-Imaging, Canada).

2.46 Aggregometry

In a total volume of 500 μ L, PRP (300×10^9 platelets/L) was incubated at 37°C for 100 minutes with peptide-conjugated HPG or native HPG at a final concentration calculated to give the I_{C50} of that material. The samples were loaded into the aggregometer (Chrono-Log, USA) and agglutination was initiated by 15 μ L of 125 mg/mL ristocetin (which is equivalent to the amount used for flow cytometry) and the aggregation curve was recorded for 6 minutes. As reference, platelet poor plasma derived from the same blood source, produced by high speed centrifugation and extruded through

a 0.20 μm filter was used. The results are represented by numerical/percentage values related to the decrease of optical diffraction (Table 3.22).

2.5 Statistical Analysis

Statistical analysis of all data to include 95% confidence intervals, two-tailed Student's t-tests, and graphics generation were performed on the Microsoft Office 2003 Excel software. Due to the volume of data, only relevant comparisons were made.

Chapter 3 – Results

3.1 HPG-RGD Conjugates

The results of this section are published (Zhang *et al.*, 2008).

3.1.1 Synthesis and Characterization of HPG-peptide Conjugates

Peptides carrying the RGD motif were conjugated to HPGs of different molecular weights (Table 1). Because the number of hydroxyl groups approximately equals the degree of polymerization, a large number of peptide moieties can be coupled to the high molecular weight HPG which are thus ideal for realizing polyvalency. It is to be noted that the hydrodynamic radii of these branched molecules increase only marginally with molecular weight and are in the range of 7-10 nm as described earlier (Kainthan *et al.*, 2006). The extent of functionalization was kept below 20 % of the total hydroxyl groups as highly deprotonated HPGs are insoluble in DMSO (Knischka *et al.*, 2000). The alkoxide groups were reacted with divinyl sulfone and the resulting vinyl sulfone end groups were utilized to couple the cysteine terminated peptides (Fig. 2.31).

The presence of phenylalanine residues in the peptide allows for the quantitative determination of the degree of substitution of the conjugate by UV spectrophotometry. The degrees of substitution were determined to be 0.05-0.1 for the 3 kDa conjugates, 125-150 for 100 kDa conjugates, and 1000-1500 for 515 kDa conjugates.

Table 3.11. Synthesis, characterization, and evaluation of RGD and RGD-HPG conjugates.

Name	HPG Platform MW	UV Spec. RGD peptides per HPG	Theoretical MW	I _{C50} (M)	[RGD] used to achieve I _{C50} (M)
HPG	3/100/515 kDa	n/a	3/100/515 kDa	No activity	n/a
RGDF	n/a	n/a	0.882 kDa	$5.0 \times 10^{-5}*$ ##	5.0×10^{-5}
C-1	3 kDa	0.11	3.1 kDa	$5.0 \times 10^{-4}*$	5.5×10^{-5}
C-2	3 kDa	0.05	3.0 kDa	$5.0 \times 10^{-3}*$	2.5×10^{-4}
C-3	100 kDa	125	210 kDa	$3.3 \times 10^{-7}†$	4.1×10^{-5}
C-4	100 kDa	151	233 kDa	$2.2 \times 10^{-7}†$	3.3×10^{-5}
C-5	515 kDa	1.01×10^3	1410 kDa	$1.2 \times 10^{-8}#$	1.2×10^{-5}
C-6	515 kDa	1.42×10^3	1770 kDa	$1.4 \times 10^{-8}#$	2.0×10^{-5}
C-7	515 kDa	1.51×10^3	1850 kDa	$1.2 \times 10^{-8}#$	1.8×10^{-5}

*, †, and # denote significant differences (p<0.05) between RGDF and its target of comparison

3.12 Effects of the Unconjugated HPG on Resting and Activated Platelets

Naked, unconjugated HPGs do not induce fibrinogen binding to platelets above control levels (Fig. 3.12), nor do they inhibit fibrinogen binding to either resting or activated platelets (Fig. 3.12). Furthermore, the RGD peptides and conjugated HPGs did not cause any platelet activation above control levels as detected by degranulation and consequent CD62 surface expression.

3.13 Effects of the Peptide Conjugated HPG on Resting Platelets

Peptide conjugated HPG increased fibrinogen binding to resting platelets in a size- and substitution-dependent manner. Free RGD peptides and smaller (3 kDa) conjugates did not increase the levels of fibrinogen bound to resting platelets; however, the larger conjugates (100 kDa and 515 kDa) significantly enhanced (p < 0.05) fibrinogen binding. This trend also applies to large conjugates in a substitution-dependent manner: platelet fibrinogen binding is increased significantly (p < 0.05) with increasing degrees of

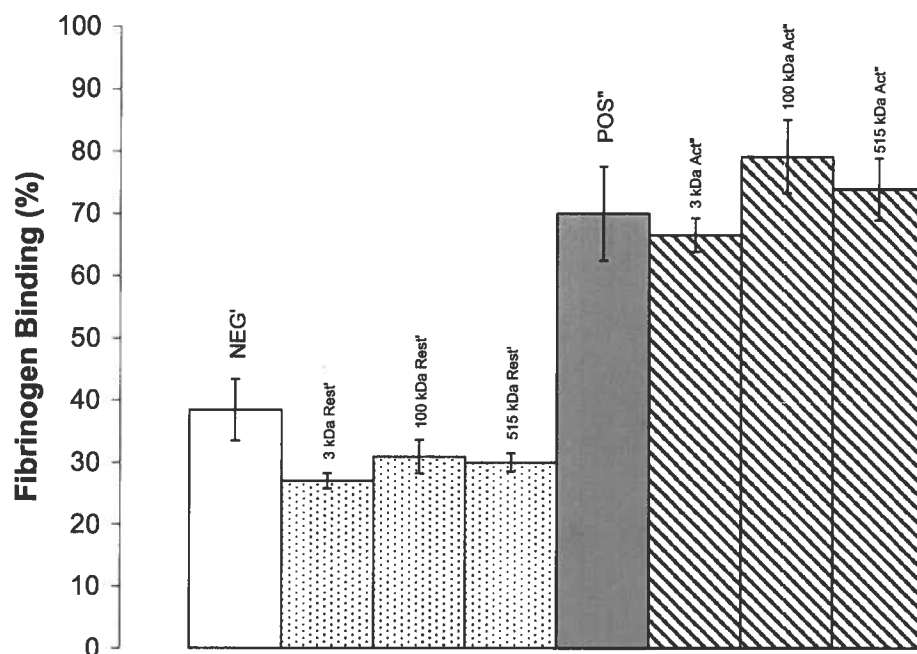


Figure 3.12. Evaluation of the Effect of Unconjugated HPGs on Resting and Activated Platelets. NEG (1): resting platelets; 3 kDa, 100 kDa, and 515 kDa Rest (Dotted histograms): resting platelets incubated with 3, 100, and 515 kDa HPG, respectively; POS (Filled histogram): Mn^{2+} activated platelets; 3 kDa, 100 kDa, and 515 kDa Act (Striped histograms): Mn^{2+} activated platelets incubated with 3, 100, and 515 kDa HPG, respectively.

‘: No significant differences were found between resting platelets and resting platelets incubated with HPG.

“: No significant differences were found between activated platelets and platelets incubated with HPG and then activated.

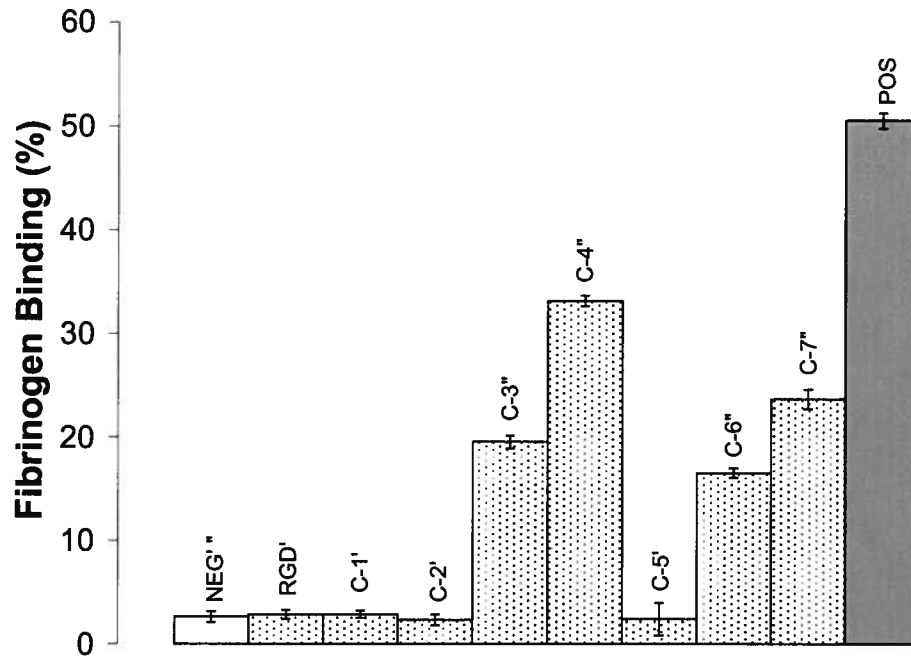


Figure 3.131. Effect of HPG-RGD Conjugates on Fibrinogen Binding by Resting Platelets. Resting platelets are incubated with RGD and various HPG-RGD conjugates. NEG: resting platelets; Dotted histograms: resting platelets incubated with RGD, C-1, C-2, C-3, C-4, C-5, C-6, and C-7 HPG-RGD conjugates at their respective I_{C50} concentrations; POS: Mn^{2+} activated platelets.

‘: No significant differences were found between resting platelets and resting platelets incubated with HPG-RGD or RGD.

‘‘: Significant differences ($p < 0.05$) were found between resting platelets and resting platelets incubated with some HPG conjugates (C-3, C-4, C-6, C-7).

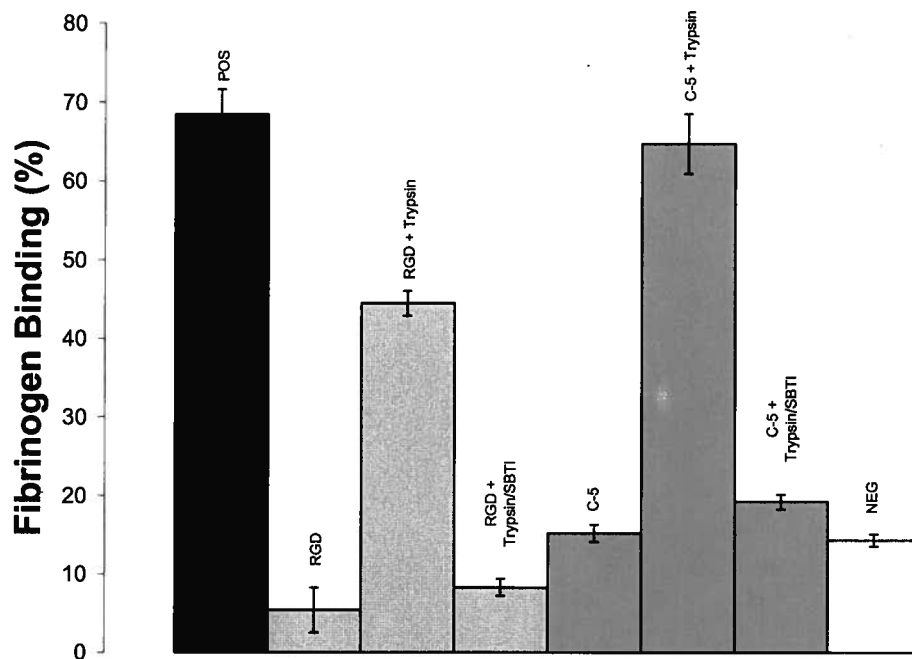


Figure 3.132 Trypsin Proteolysis Assays of RGD and HPG-RGD Conjugates.

Histogram 1 (POS): positive control, ADP activated platelets; Histogram 2 (RGD): platelets incubated with RGD at I_{C50} and activated with ADP; Histogram 3 (RGD + Trypsin): platelets incubated with tryptic digest of RGD peptides and activated with ADP; Histogram 4 (RGD + Trypsin/SBTI): platelets incubated with SBTI inhibited tryptic digest of RGD peptide and activated with ADP; Histogram 5 (C-5): platelets incubated with C-5 HPG-RGD conjugate at I_{C50} and activated with ADP; Histogram 6 (C-5 + Trypsin): platelets incubated with tryptic digest of C-5 HPG-RGD conjugate and activated with ADP; Histogram 7 (C-5 + Trypsin/SBTI): platelets incubated with SBTI inhibited tryptic digest of C-5 HPG-RGD conjugate peptide and activated with ADP. Histogram 8 (NEG): negative control, resting platelets (unactivated). Tryptic cleavage of RGD significantly ($p < 0.05$) decreased RGD and HPG-RGD conjugate's activity.

substitution by RGD peptides (Fig. 3.131). Tryptic removal of the RGD conjugated to the HPG produced significant ($p < 0.05$) decreases in inhibitory activity of the HPG-RGD conjugates and confirmed that the inhibition of fibrinogen binding was RGD-dependent (Fig. 3.132).

3.14 Effects of the Conjugated HPG on Activated Platelets

Conjugated HPGs' inhibition of fibrinogen binding to platelets is concentration-, size- and substitution-dependent. This was true especially for the 100 kDa and 515 kDa conjugates (Fig. 3.14). That this inhibition was specific and required the presence of the RGD motif was confirmed by the loss of function after enzymatic removal of the RGD (Fig. 3.132). Based on the titration curves, I derived I_{C50} values that are shown in Table 3.11. Significant differences ($p < 0.05$) were observed between 3 kDa conjugates, 100 kDa conjugates, 515kDa conjugates, and RGD. No statistically significant differences were found within the groups. The mathematical relationship between HPG size, substitution, and resultant I_{C50} is summarized in Figure 3.15: I_{C50} can be reduced with an increase in the molecular weight of HPG as well as an increase of the RGD substitution ratio. The range of Figure 3.15 is exaggerated beyond experimental data in order to further extrapolate current findings.

3.15 Macroscopic Platelet Aggregation

In general, both the free RGD peptides and the RGD-conjugated HPG inhibited agonist-induced, macroscopic platelet aggregation whether the aggregation was assessed visually via light microscopy or semi-quantitated by lumiaggregometry (Table 3.12, Figure 3.16). I also found that HPG-RGD conjugates do not cause spontaneous platelet

aggregation of resting platelets as could have been suggested by the increased fibrinogen binding by platelets incubated with conjugates of high substitution (C-7).

Table 3.12. Light microscopy of RGD-HPG conjugates and aggregation of resting and Mn^{2+} activated platelets in the presence of free RGD peptides and RGD-HPG conjugates at their respective I_{C50} values.

Assay	Microscopy of Visible Aggregates		Aggregometry
	Resting Platelets	Mn^{2+} Activated Platelets	% Aggregation
Negative Control	-----	-----	1
Positive Control	+++++		70
RGDF	-----	-----	5
C-1	-----	-----	5
C-2	-----	-----	5
C-3	-----	-----	5
C-4	-----	-----	5
C-5	-----	-----	5
C-6	-----	-----	10
C-7	-----	-----	5

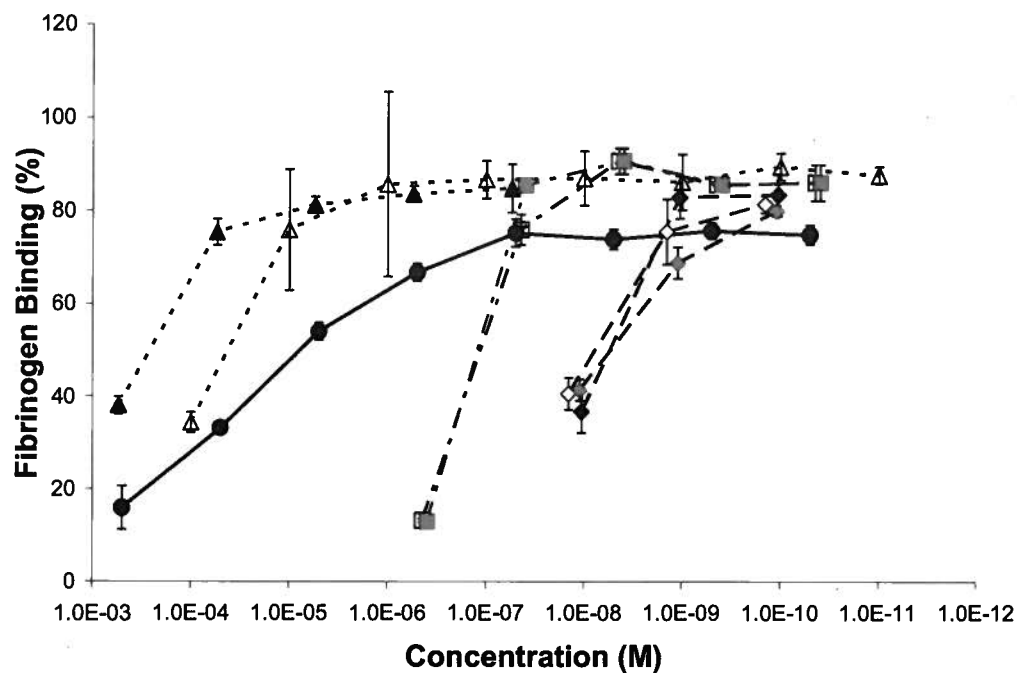










Figure 3.14. Inhibitory Effects of HPG-RGD Conjugates on Platelet-Fibrinogen Binding. Platelets are incubated with RGD or HPG conjugates and fibrinogen at varying concentrations and activated with Mn^{2+} . RGD:  ; 3 kDa HPG conjugates are marked with triangles and dotted lines: C-1:  ; C-2:  ; 100 kDa conjugates are marked with squares and dashed lines with dots in between: C-3:  ; C-4:  ; 515 kDa conjugates are marked with diamonds and dashed lines: C-5:  ; C-6:  ; C-7: .

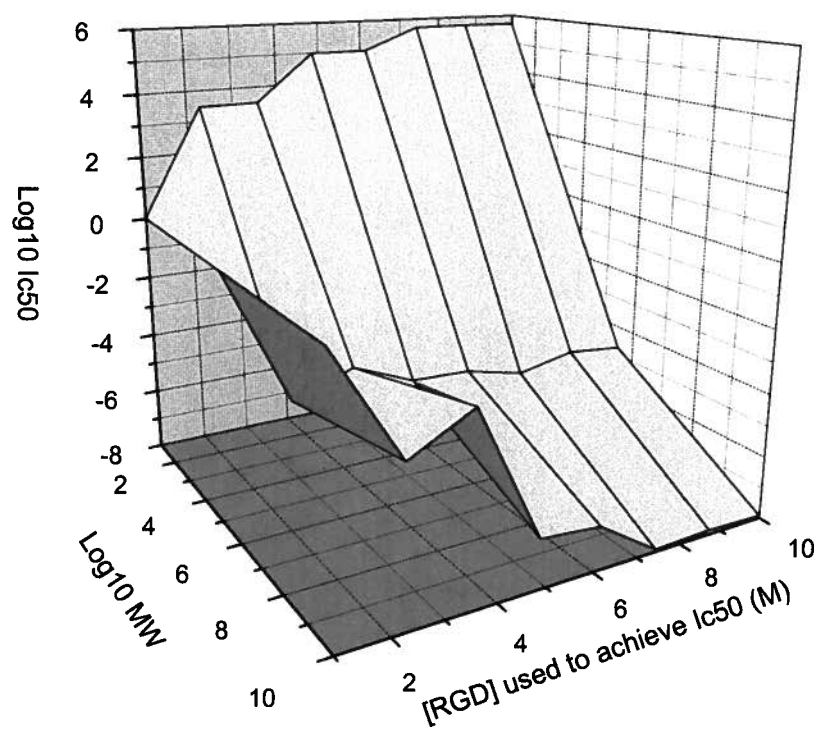


Figure 3.15. Relationships Among I_{C50}, HPG Polymer Molecular Weight and Amount of RGD Peptides Conjugated to HPG. Parameters are plotted on logarithmic scales, the graphed range covers areas that exceed experimental data and are meant to be there as interpolated representations. High RGD substitution ratios and high HPG molecular weight serve to reduce I_{C50}.

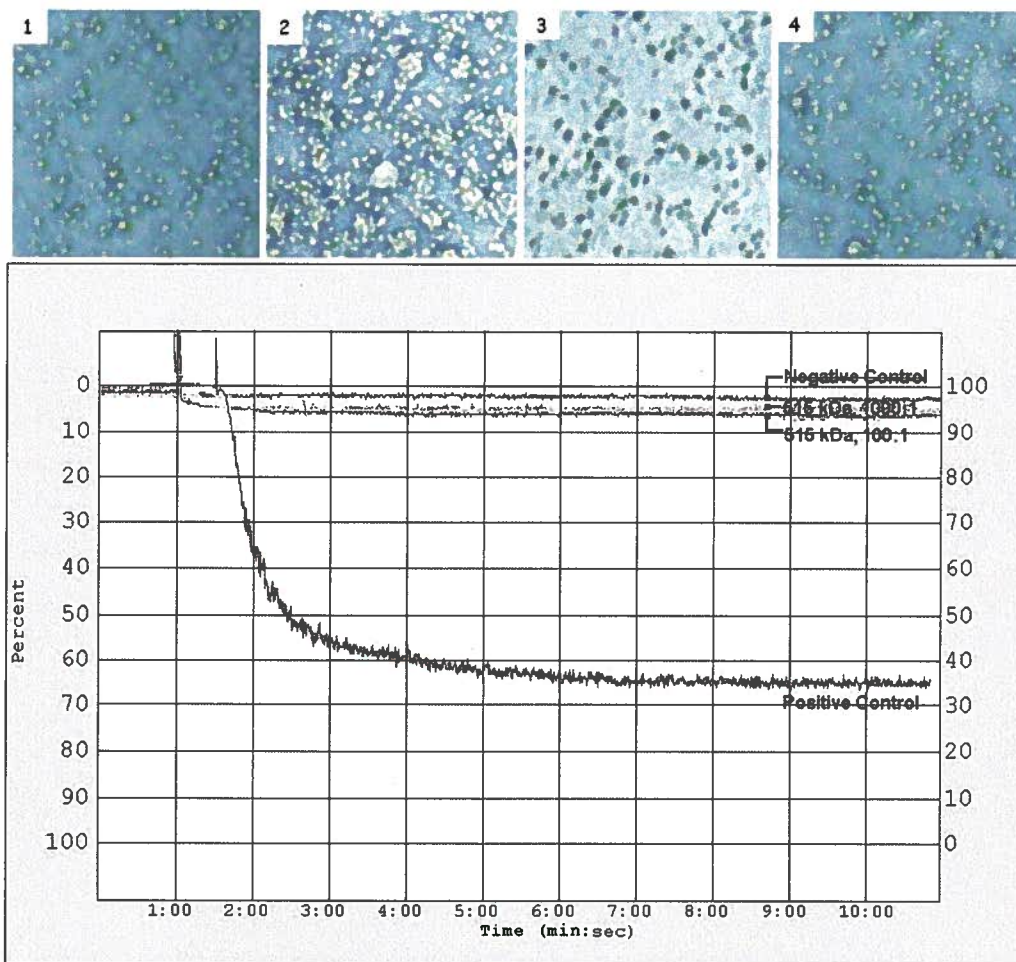


Figure 3.16. Light Microscopy and Aggregometry.

Compound Light Microscopy 400×, Panel 1: Resting platelets, Panel 2: Mn^{2+} Activated platelets, Panel 3: Mn^{2+} activated platelets incubated in C-5 HPG-RGD, Panel 4: Mn^{2+} activated platelets incubated with C-7 HPG-RGD.

Aggregometry Graph, Negative control: resting platelets, Positive control: Mn^{2+} activated platelets, C-5 HPG-RGD: platelets incubated with RGD conjugate and activated with Mn^{2+} , C-7 HPG-RGD: platelets incubated with RGD conjugate and activated with Mn^{2+} .

*This figure is used only as a visual reference for data represented in tables, and will not be described in subsequent sections of the thesis.

3.2 HPG-SHAYIGLKDR Conjugates

The Results of this section are being drafted for publication.

3.21 Synthesis and Characterization of Peptide-conjugated HPG

HPG was first derivatized with divinyl sulfone (DVS) to allow for subsequent peptide attachment. For the targeted 10:1 DVS to HPG ratio, the actual HPG-bound vinyl sulfone (HPG-VS) was calculated to be 9.75:1 by the back-titration thiol-estimation assay. Similarly, a ratio of 99:1 was obtained for the targeted 100:1 DVS to HPG, suggesting that the vinyl sulfone groups were the limiting condition for conjugation as they were saturated by the peptides. Furthermore, there appeared to be no steric interference among the peptide molecules themselves that would interfere with their conjugation to the HPG carrier.

Because excess peptide conjugation was at a level sufficient to saturate the vinyl sulfone groups, thiol-estimation was not used to quantify the peptides on the peptide-HPG constructs. Instead, the peptide's native tyrosine residue's UV absorbance was exploited as a measure conjugation using the molar extinction coefficient of $1260 \text{ M}^{-1} \text{ cm}^{-1}$ at 278 nm. 10:1 conjugates (L_{10} to DR_{10}) were found to have approximately 9.5 peptides per HPG, and 100:1 conjugates (L_{100} to DR_{100}) were found to have approximately 96 peptides per HPG. This confirmed the near complete or complete reaction of the HPG-VS with excess peptide (Table 3.21).

3.22 Effects of the Native HPG and Peptide-conjugated HPG on Resting Platelets

Degranulation, a part of the amplification pathway of platelet signalling during activation, exposes CD62/P-selectin on platelet surfaces such that CD62 quantitation is a useful biomarker for platelet activation. Native, unconjugated HPG, free

Table 3.21. Functionalization and Characterization of HPG and HPG conjugates.

Name	HPG Platform MW	DVS per HPG	Peptides per HPG	Theoretical MW	I _C 50 (M)	[Peptide] used to achieve I _C 50 (M)
HPG	---	---	---	500 kDa	No activity	0
L-pep	---	---	---	1.605 kDa	$4.8 \pm 0.6 \times 10^{-5} * \# \text{¥}$	4.8×10^{-5}
LR-pep	---	---	---	1.605 kDa	$3.4 \pm 0.3 \times 10^{-5} * \dagger \gamma$	3.4×10^{-5}
D-pep	---	---	---	1.605 kDa	No activity	No activity
DR-pep	---	---	---	1.605 kDa	No activity	No activity
L ₁₀	500 kDa	9.8 ± 0.1	10 ± 1	516 kDa	$6.7 \pm 0.3 \times 10^{-6} \#$	6.7×10^{-5}
LR ₁₀	500 kDa	9.8 ± 0.1	10 ± 1	516 kDa	$4.1 \pm 0.7 \times 10^{-6} \dagger$	4.1×10^{-5}
D ₁₀	500 kDa	9.8 ± 0.1	10 ± 1	516 kDa	No activity	No activity
DR ₁₀	500 kDa	9.8 ± 0.1	11 ± 1	518 kDa	No activity	No activity
L ₁₀₀	500 kDa	98 ± 2	113 ± 10	680 kDa	$1.1 \pm 0.5 \times 10^{-6} \text{¥}$	2.1×10^{-4}
LR ₁₀₀	500 kDa	98 ± 2	107 ± 10	671 kDa	$4.9 \pm 0.5 \times 10^{-7} \gamma$	2.2×10^{-5}
D ₁₀₀	500 kDa	98 ± 2	93 ± 9	649 kDa	No activity	No activity
DR ₁₀₀	500 kDa	98 ± 2	93 ± 9	649 kDa	No activity	No activity

*, †, #, ¥, and γ denote $p < 0.05$ between the pairs.

Table 3.22. Light Microscopy, Aggregometry, and Flow Cytometry of HPG

conjugates with Resting and/or Activated platelets

Assay	Microscopy of Visible Aggregates		Aggregometry	CD62 Surface Expression		vWf-binding
	Resting Platelets	Activated Platelets		Resting Platelets	Activated Platelets	
Negative Control	-----	+++	5 ± 5	$22 \pm 2^*$	30 ± 2	$20 \pm 3'$
Positive Control	+++		80 ± 5	90 ± 2	$78 \pm 5''$	99 ± 1
HPG	-----	+++	76 ± 5	$22 \pm 1^*$	$74 \pm 4''$	$26 \pm 5'$
L-pep	-----	-----	5 ± 5	$18 \pm 1^*$	$72 \pm 8''$	$24 \pm 4'$
LR-pep	-----	-----	5 ± 5	$19 \pm 2^*$	$70 \pm 5''$	$25 \pm 12'$
D-pep	-----	+++	80 ± 5	$18 \pm 2^*$	$68 \pm 10''$	$14 \pm 8'$
DR-pep	-----	+++	78 ± 5	$27 \pm 18^*$	$72 \pm 3''$	$28 \pm 3'$
L ₁₀	-----	-----	5 ± 5	$17 \pm 1^*$	$73 \pm 5''$	$22 \pm 5'$
LR ₁₀	-----	-----	5 ± 5	$17 \pm 2^*$	$72 \pm 4''$	$24 \pm 2'$
D ₁₀	-----	+++	82 ± 5	$14 \pm 7^*$	$70 \pm 6''$	$24 \pm 2'$
DR ₁₀	-----	+++	80 ± 5	$19 \pm 1^*$	$72 \pm 7''$	$30 \pm 3'$
L ₁₀₀	-----	-----	5 ± 5	$20 \pm 3^*$	$71 \pm 5''$	$23 \pm 2'$
LR ₁₀₀	-----	-----	5 ± 5	$18 \pm 1^*$	$73 \pm 2''$	$22 \pm 2'$
D ₁₀₀	-----	+++	73 ± 5	$18 \pm 1^*$	$72 \pm 1''$	$26 \pm 3'$
DR ₁₀₀	-----	+++	70 ± 5	$19 \pm 1^*$	$75 \pm 3''$	$18 \pm 6'$

*, '', ': no significant differences were found within these groups.

peptidomimetics, and peptide-conjugated HPG in contact with resting platelets do not cause platelet activation as detected by CD62 surface expression (Table 3.22). In addition, HPG do not increase vWf binding to resting platelets (Table 3.22), which could trigger vWf crosslinking, platelet activation, or both.

3.23 Effects of the Peptide-conjugated HPG on Activated Platelets

Peptide-conjugated HPGs' inhibition of vWf binding to platelets was concentration- and substitution-dependent (Fig. 3.231). The D-enantiomer based peptides and their conjugates showed no inhibitory activity while both the L and the L-Reverso peptides as well as their conjugates (L₁₀, LR₁₀, L₁₀₀, LR₁₀₀) proved to be effective inhibitors. The free L-Reverso peptide was a significantly better inhibitor ($p < 0.05$) of the GPIb-vWf interaction than the native L-peptide. However, this was not true for the conjugated forms (Table 3.21). Based on the titration curves (Figure 3a), and the I_{C50} values determined from them (Table 3.21), the peptides' inhibitory effectiveness was augmented by as much as two orders of magnitude ($p < 0.05$) by their conjugation to HPG.

The materials did not inhibit platelet activation by thrombin as measured by CD62 surface expression. This confirms that the HPG-conjugates interfere solely with platelet activation mechanisms through GPIb-vWf and that the inhibitory activities of the HPG-peptide conjugates are specific. This is further underlined by the fact that neither the native HPG nor the free peptides, nor combinations thereof are sufficient for inhibition. The presence of the peptidomimetic motif on the HPG is a requirement, as the loss of this function after trypsin cleavage removes the function of the conjugates (Figure 3.232).

Further, neither the L-peptide nor its conjugate L₁₀₀ were found to induce direct GPIb dependent platelet activation of resting platelets. This is demonstrated both by the lack of increase of CD62 expression/platelet degranulation shown in Table 3.22 as well as by GPIIbIIIa activation of resting platelets treated with these substances (Figure 3.233). Ristocetin treatment to induce platelet activation (CD62 expression/GPIIbIIIa activation) through the GPIb dependent signalling pathway *via* activation of vWf also failed to cause GPIIbIIIa activation of platelets incubated with L-peptide and L₁₀₀ (Figure 3.233).

3.24 Macroscopic Platelet Aggregation

The inhibition of platelet agglutination by vWf was observed both by light microscopy and lumiaggregometry. No clumping was seen when resting platelets were incubated with free peptides, native HPG, or peptide-conjugated HPG (Table 3.22). To show inhibition of the GPIb-vWf interaction in PRP, activation must target the plasma component, specifically vWf, by ristocetin rather than by platelet activators such as thrombin (Table 3.22). Platelets did not agglutinate in the presence of ristocetin if they had been incubated with either the peptides or the peptide-conjugated HPG at their respective I_{C50} concentrations.

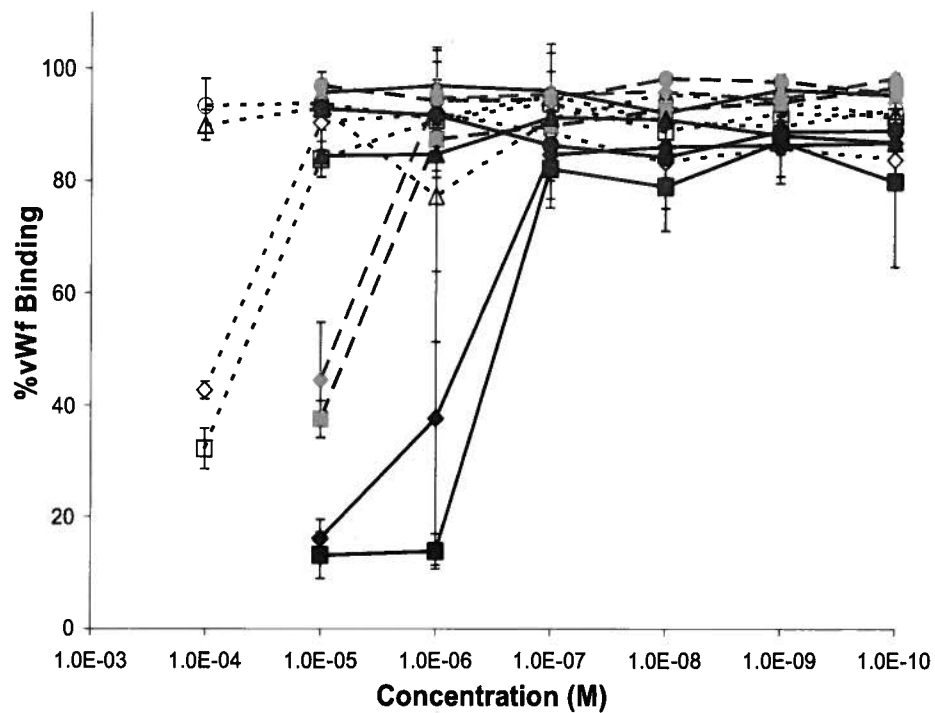


Figure 3.231. Inhibition of Platelet-vWf Binding by Peptide-conjugated HPG PRP

platelets incubated with either peptides or conjugates are activated by ristocetin and

assessed for vWf binding under flow cytometry (FACS Canto II). L-peptide: ◇, LR-

peptide: □, D-peptide: ○, DR-peptide: △, L₁₀: ◊, LR₁₀: ◻, D₁₀:

●, DR₁₀: ▲, L₁₀₀: ◆, LR₁₀₀: ◼, D₁₀₀: ●, DR₁₀₀: ▲.

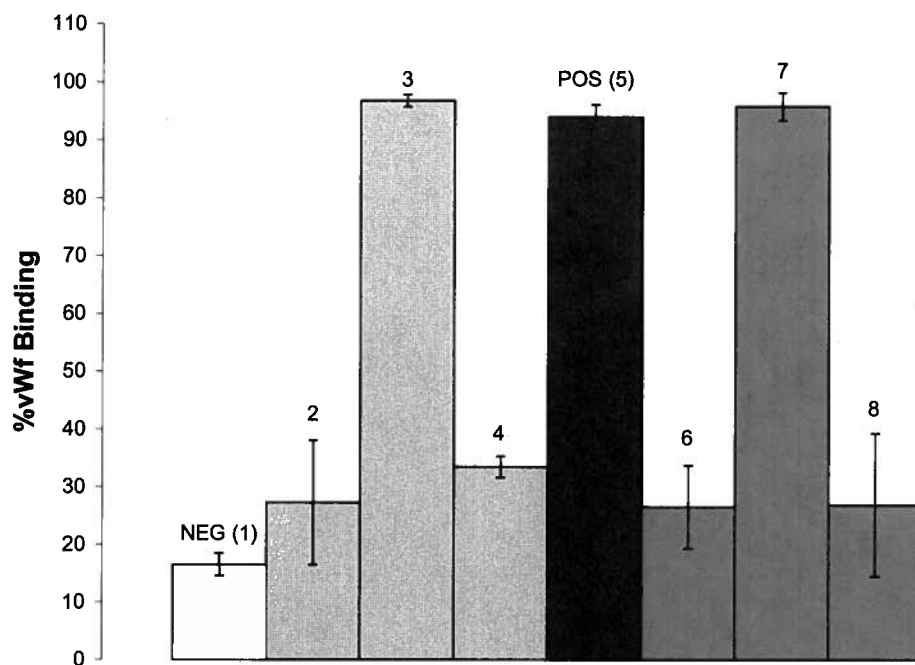


Figure 3.232. Trypsin Proteolysis Assays of SHAYIGLKDR and HPG-SHAYIGLKDR Conjugates. Histogram NEG (1): PRP platelets are checked for baseline vWf binding. Histogram 2: platelets incubated with LR-peptide at I_{C50} and treated with ristocetin. Histogram 3: platelets incubated with trypsin digested LR-peptide and treated with ristocetin. Histogram 4: platelets incubated with SBTI inhibited trypsin digested LR-peptide and treated with ristocetin. Histogram POS (5): Platelets treated with ristocetin. Histogram 6: platelets incubated with LR₁₀₀ conjugate at I_{C50} and treated with ristocetin. Histogram 7: platelets incubated with trypsin digested LR₁₀₀ conjugate at I_{C50} and treated with ristocetin. Histogram 8: platelets incubated with SBTI inhibited trypsin and treated with ristocetin.

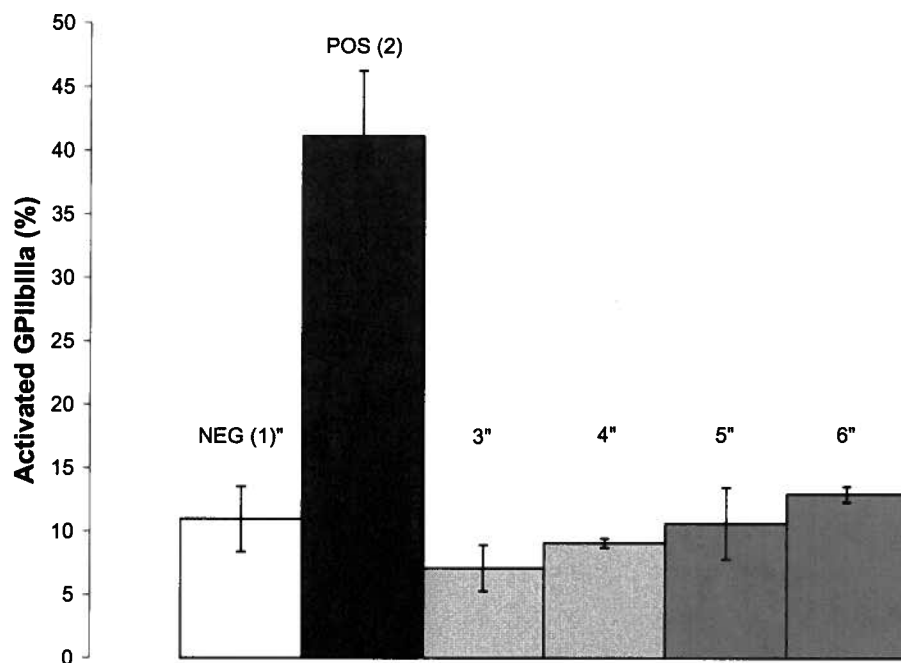


Figure 3.233. Effect of Peptide on GPIIb/IIIa Activation Through GPIb Signalling.

Histogram NEG (1): resting platelets are checked for baseline GPIIb/IIIa activation. Histogram POS (2): resting platelets treated with ristocetin. Histogram 3: resting platelets treated with L-peptide at I_{C50} . Histogram 4: resting platelets treated with L_{100} conjugate at I_{C50} . Histogram 5: resting platelets treated with L-peptide at I_{C50} and activated with ristocetin. Histogram 6: resting platelets treated with L_{100} at I_{C50} and activated with ristocetin.

“: No significant differences were found among resting platelets and ristocetin-activated platelets under peptide or conjugate suppression.

Chapter 4 – Discussion

4.1 HPG-RGD Conjugates

The attachment of RGD peptides to HPG confers unique attributes to the resulting construct: the HPG gains specificity and thereby function while the peptidomimetic gains polyvalency and thereby binding avidity.

4.11 Characterization

Peptide attachment increases the theoretical molecular weight of the HPG-conjugates depending on the number of available sites that can be functionalized on the surface of the HPG polymer. The branch density of the HPG varies directly with the molecular weight of the polymer while the Stokes' radius of the molecule remains relatively stable at about 7-10 nm for the 100 kDa and 515 kDa HPG molecules (Kainthan *et al.*, 2006). The peptidomimetic is predicted to be <1 nm in length, thus based on the level of substitution, peptide conjugation can approximately triple the theoretical MW of the 515 kDa HPG polymer to up to 1850 kDa for the HPG-RGD conjugate. Since attachment of the peptides is through divinyl sulfone, a reaction with limiting yields and kinetics (compared to DVS attachment to HPG), it is not surprising that the 3 kDa HPG (C-1 and C-2) carried few RGD peptides after conjugation. The achieved peptide density has steric implications for subsequent function due to its polyvalent binding to multiple GPIIb/IIIa receptors on the platelet surface.

The design of the peptide included an N-terminal cysteine for attachment and five glycine residues to facilitate the RGD motif's access to the GPIIb/IIIa binding pocket (Beer *et al.*, 1992). The RGDF sequence was considered by Foster *et al* (Foster *et al.*,

2003) to be the most potent of the small RGD-peptidomimetics ($IC_{50} = 8 \times 10^{-3}$ M) and the phenylalanine was also useful for detection UV tracking of the peptide (Foster *et al.*, 2003).

4.12 Function

In order to evaluate whether RGD-conjugated HPGs have specific interactions with platelets, the range of MW of naked, unconjugated HPG were examined first. Both the original studies (Kainthan *et al.*, 2007; Kainthan & Brooks, 2007) and the assays presented here involving either resting or activated platelets show no significant alterations of fibrinogen binding to platelets. Although plasma fibrinogen concentration, platelet surface GPIIb/IIIa levels and degree of preparation-induced platelet activation vary with the individual, similar IC_{50} values were obtained with the plasma and cells of all the blood donors tested. Furthermore neither the unconjugated HPG nor the RGD-conjugated HPG induced platelet activation as defined by degranulation and CD62 expression. However, the RGD-conjugated HPG promoted some fibrinogen binding to resting platelets in a manner that could be related to both HPG molecular size and degree of RGD substitution: the dense RGD brushes on HPG increased fibrinogen binding to platelets more than the diffuse RGD brushes. This can be attributed to the cooperativity of GPIIb/IIIa binding of RGD motifs such that RGD binding to a GPIIb/IIIa receptor enhances the ability of other GPIIb/IIIa molecules to bind fibrinogen (Bassler *et al.*, 2007; Dickfeld *et al.*, 2001).

The most important finding was that fibrinogen binding to activated platelets, and subsequent platelet aggregate formation is inhibited by RGD-conjugated HPG in a manner related to HPG size (Fig. 3.14), and to its degree of substitution (Fig. 3.14). As

the 3 kDa conjugates carried few RGD peptides, higher concentrations were needed to achieve the same degree of inhibition as obtained for free RGD peptides. However, both the 100 kDa and 515 kDa HPG conjugates carry 100 - 1500 RGD peptides, and thus they are able to reduce the I_{C50} of free RGD peptides by two to three orders of magnitude. Extrapolating from this data (Fig. 3.15), it is possible to derive the substitution/MW relationship to achieve optimal platelet inhibition.

The large decrease of the I_{C50} and the corresponding increase of the HPG-conjugated RGD peptides' inhibitory effect may be a matter of kinetics. As a result of the polyvalent presentation of the RGD conjugated to HPG (Figure 4.11), the binding of RGD to platelet GPIIb/IIIa is enhanced due to both a higher local concentration of RGD peptides, and a slowed dissociation due to several concurrent dynamic associations of HPG-RGD with two or more GPIIb/IIIa integrins (Figure 4.12). As well, there is cooperativity among GPIIb/IIIa receptors, such that a single bound RGD changes the GPIIb/IIIa conformation to increase the likelihood of further ligand binding (Bassler *et al.*, 2007; Dickfeld *et al.*, 2001).

It is known that free RGD peptides can activate the GPIIb/IIIa receptors such that an increased number of the receptors remain in the "open" configuration that is capable of binding fibrinogen. (Bassler *et al.*, 2007; Dickfeld *et al.*, 2001) Thus it is not unlikely that the HPG-carried RGD generate a similar activating effect. Increased fibrinogen binding seen on flow cytometry of resting platelets is caused by high molecular weight, high substitution HPG-RGD. However, this fibrinogen binding does not seem to cause spontaneous platelet macroscopic aggregation, as observed *via* light microscopy and lumiaggregometry. The conjugates however, still inhibit the macroscopic aggregation of

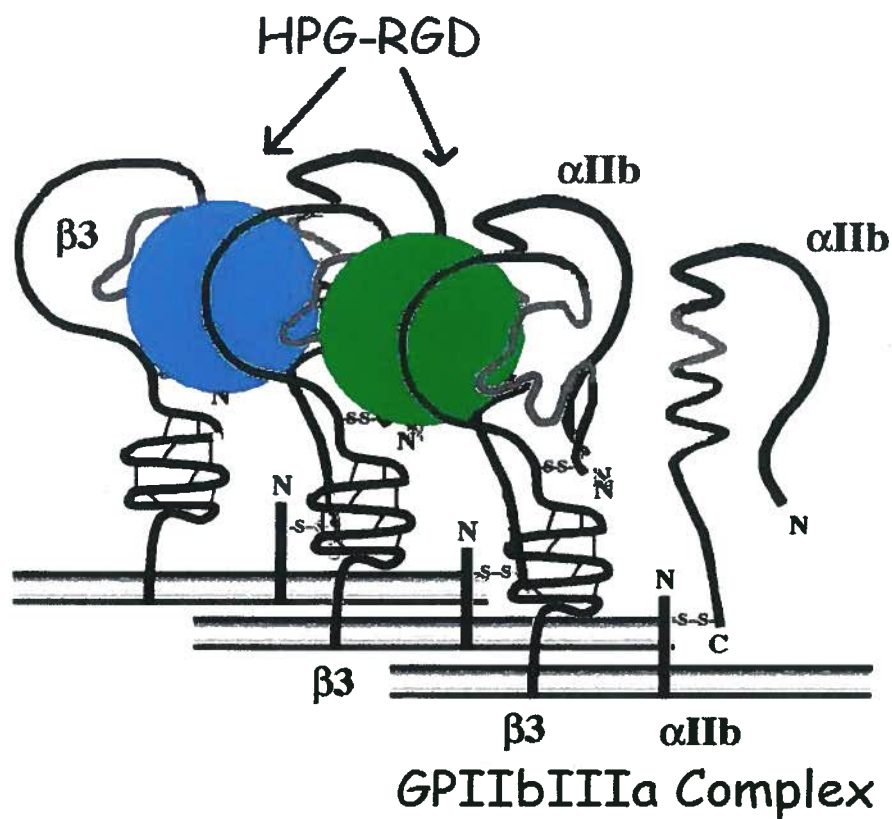


Figure 4.11. Proposed Mechanism A: Polyvalency of HPG-RGD Conjugates. Simultaneous binding to multiple GPIIb/IIIa receptors on platelet surfaces by a corresponding number of RGD peptides attached to HPG resulting in significantly reduced dissociation kinetics. Differential color label (blue and green) for the HPG-RGD conjugates denote the conjugates as a heterogeneous population.

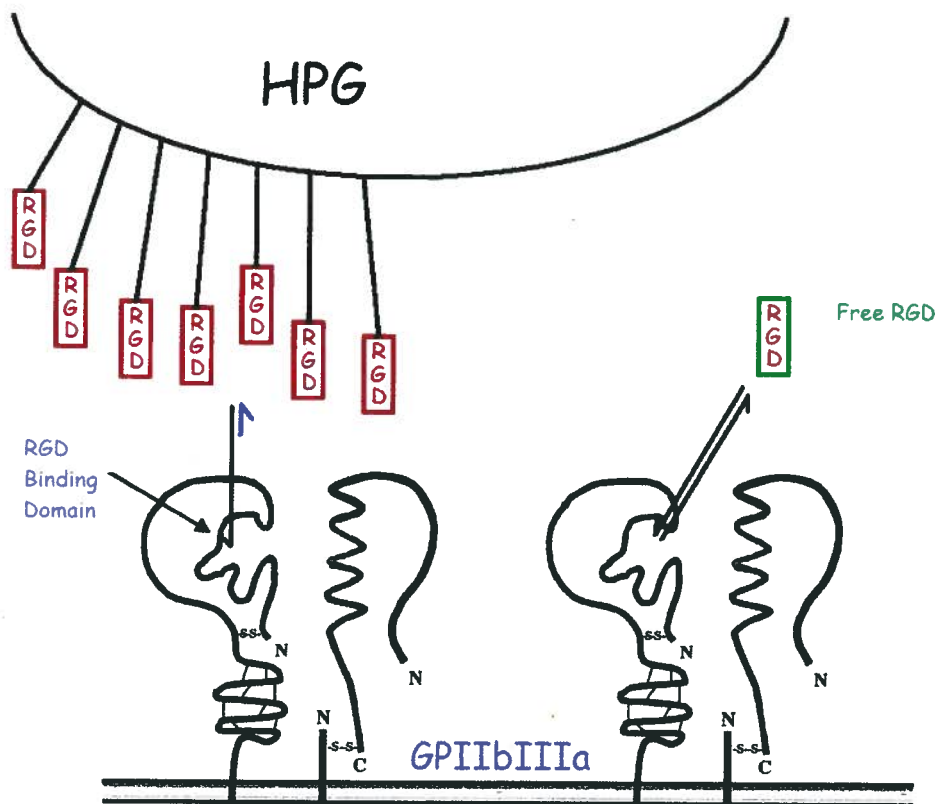


Figure 4.12. Proposed Mechanism B: Higher Local Concentration. Increased availability of RGD molecules brought by HPG shifts the equilibrium towards binding association with platelet surface integrin GPIIb/IIIa. Red, up-side-down flag-like objects denote RGD peptides.

Mn²⁺ activated platelets as detected both macroscopically (Fig. 3.16, Table 3.12) and by flow cytometry (Fig. 3.14).

Figure 3.15 demonstrates the mathematical relationship between I_C50, substitution ratio, and HPG molecular weight. We see that an increase in substitution and HPG molecular weight causes a decrease in I_C50. Base on Figure 3.15 it would seem that we should use 515 kDa HPG with 1000:1 substitution ratio. However, this construct causes platelets to spontaneously bind platelets as well as the same molecular weight with 500:1 substitution ratio (Figure 3.131). As a result, the 500 kDa HPG with lower conjugation ratios (10:1 and 100:1) were chosen and the results are discussed in the following section.

4.2 HPG-SHAYIGLKDR Conjugates

4.21 Peptide Selection

Here, the peptidomimetic peptide is a native sequence of the vWf molecule selected by probing on a tandem peptide array. The peptide binds at or near the GPIb active site for vWf, but does not spontaneously trigger platelet activation either through GPIb. Neither are CD62 expression/degranulation (Table 3.22) and GPIIb/IIIa activation triggered (Figure 3.233), but GPIb-dependent platelet activation is inhibited (Figure 3.231, Figure 3.233): this is defined as a dominant-negative peptide (Kirchmaier & Sugden, 1997).

4.22 Choice of Platform and Linker

We chose the 500 kDa HPG molecule as the platform because for higher molecular weight polymers molecular size increases only modestly with increasing

molecular weight (Kainthan *et al.*, 2006). Based on the data from Figure 3.15 and Table 3.11, we had determined that the number of peptides attached to HPG is vital to the level of enhancement of peptide activity. The 500 kDa HPG molecules have the highest density of branches and hence the most number of available hydroxyl groups for conjugation. Peptides were again attached to HPG through a terminal cysteine sulfhydryl's side chain in a thiol-selective manner using divinyl sulfone (Houen *et al.*, 1995; Bulmus *et al.*, 2000).

The peptidomimetic was designed to contain a cysteine in the linker moiety (Zhang *et al.*, 2008) *ie* the 7-mer peptide linker: CGGGGGG described in this study. In the design of the linker, considerations that become important include length, composition, and polarity, as well as the inclusion of reactive groups for conjugation. The linker length and composition may adversely affect the peptide's activity if an inadequate length prevents access of the peptide to the GPIIb receptor's binding site. Based on previous studies (Zhang *et al.*, 2008), we somewhat arbitrarily decided to lengthen the linker to 7 glycines to allow for increased flexibility in order to be able to attach to the linear binding domain of GPIIb. Conjugation to a macromolecule, whether with or without a linker, fixes the spatial orientation of the peptidomimetic. Both attachment and the addition of linkers bring peptide sequence and polarity into question as the direction of peptide binding may be an important component of that peptide's activity. Therefore, forward and reverse variations of the L-amino acid sequence were made. As well, the peptides were synthesized using non-natural D-amino acids in order to determine the relevance to the GPIIb-vWf binding activity of both the peptide bond and side chain orientation.

4.23 Characterization

Peptide attachment increases the theoretical molecular weight of the HPG-peptide conjugates: this is relative to the number of available sites for attachment as well as the number of peptides attached. The conjugation of DVS to HPG is clearly characterized by the thiol-estimation assay, which indicates a near complete reaction, attaining greater than 95% of the targeted conjugation ratio (Table 3.21). It should be noted that side reactions that polymerize HPG result in large insoluble clumps but are filtered away. The Stokes Radius of the 500 kDa naked HPG is around 8 to 10 nm by dynamic light scattering experiments (Kainthan *et al.*, 2006), and with the 17-mer peptide (calculated to be ~1-2 nm), brings the final conjugate size to 10 to 11 nm.

The terminal cysteine residues and the six glycine linkers respectively, allow conjugation to HPG-VS (Figure 3.22) and freedom for the peptidomimetic end to bind the vWf binding domain of GPIb. The tyrosine within the peptidomimetic allows quantification of the final conjugate constructs. Although other wavelengths (274 nm) may be better for tyrosine-dependent absorbance measurements, the A278 molar extinction coefficient is certainly comparable and hence it is utilized here.

4.24 Function

HPG was found to be biocompatible in past studies involving both *in vitro* and *in vivo* methods (Kainthan *et al.*, 2006; Kainthan *et al.*, 2007; Kainthan & Brooks, 2007), but its interactions specifically with platelet integrins remains unknown. A study by our group has indicated that naked HPG does not affect fibrinogen binding to either resting or activated platelets (Zhang *et al.*, 2008). Here we showed that naked HPG does not

contribute to vWf binding in resting or activated platelets (Table 3.22), as it does not seem to activate vWf or bind to the GPIb-vWf interactive domain on its own.

Neither the peptide-derivatized HPG conjugates nor the peptidomimetic peptides themselves promote vWf binding to resting platelets (Table 3.22); nor do they activate platelet GPIb, to contribute to platelet outside-in signalling as determined by CD62 surface expression (Table 3.22) and GPIIb/IIIa activation (Figure 3.233). These conjugates do not interfere with thrombin stimulated platelet activation, and thus seem to block only the GPIb-vWf dependent signalling (Table 3.22, Figure 3.231, Figure 3.233). However, it is evident that these peptides and conjugates interfere with vWf binding to platelets (Figure 3.231, Table 3.22) in a concentration- and substitution-dependent manner. This inhibitory effect can be attributed directly to the peptidomimetic peptide itself as proteolytic digestion of the peptides with trypsin causes a loss of activity (Figure 3.232). Significant differences ($p < 0.05$) were observed between the inhibitory activities of the L- and L-Reverso peptides but not between the peptide conjugated to their carrier. The D-peptides, DR-peptides, and their conjugates showed no activity. However, it should be noted that the difference in I_{C50} between the L and the LR-peptides are quite small and are on the borderline of significance and hence the loss of this difference is assumed to become negligible after conjugation. The lack of inhibitory function by D peptides is intuitive as the original peptide array is based on an L-enantiomer design while the targeted GPIb-vWf binding sequence is relatively linear.

The inhibitory effects of both the peptides and the HPG-peptide conjugates in the presence of ristocetin activated platelets is substantiated by macroscopic evidence viewed

by the compound light microscope and by aggregometry, where an absence of the agglutination response is seen (Table 3.22).

The attachment of peptidomimetic peptides to HPG confers unique attributes to the resulting construct: the HPG gains specificity and function; while the peptidomimetic gains polyvalency and binding avidity. It should be noted that although the IC_{50} of the peptidomimetic peptide itself is not very high, it remains very clear that drug conjugation to macromolecular carriers is a valuable new method to increase the effectiveness and most probably increase the *in vivo* retention of small drug molecules. In this set of experiments, we observe the same inverse linear relationship between IC_{50} and the substitution ratio of the peptidomimetic, that is, HPG-peptide conjugates carrying 100 peptides necessarily lower the IC_{50} by approximately the same amount. We have also found no difference between the forward and reverse versions of our peptidomimetic, which suggests that conjugation defined directional polarity does not affect function in this particular case where the interactive domain is linear. Since the effectiveness (IC_{50}) of the peptides attached to HPG do not differ significantly from that the peptides in their free form, we classify the interaction as polyvalency dependent. This may be a result of higher loading rates of the conjugate due to higher local concentrations and lower off-loading rates as a result of accumulated attachment to multiple GPIb receptors.

4.3 Summary

We see that the HPG conjugates' activities are modulated by the number of peptides attached to the carrier HPG. Higher molecular weight HPGs have more groups that can be functionalized on their surface and hence have the highest potential for drug enhancement. However, high conjugation ratios could increase the peptide density on the

HPG surfaces to a point where the peptides' mobility is reduced and steric hindrance to binding their receptor target becomes significant, and activity could be lost. This is perhaps a more dominant issue when considering receptors with complex internal active sites such as GPIIbIIIa, although in this study we did not seem to have approached this limit. These possibilities may not affect the vWf mimic as significantly because the binding domains are relatively linear and highly exposed. At the same time, the linker/spacer composed of poly-glycines could be either lengthened or shortened and other biocompatible materials such as poly(ethylene)glycol (PEG) can be used. The longer the linker, the more space the tips of the peptides (the active end) have to maneuver and attach to targeted sites (Figure 1.5). An optimum linker length may be titrated for binding specific receptors.

Conjugation of small molecular species to macromolecules increases the molecular weight of the resulting species, and could decrease chemical kinetics. However, an increased local concentration of peptides (Figure 4.12) as a result of high conjugation ratios and polyvalency of the HPG-peptide attachment to receptors (Figure 4.11) are able to enhance the binding kinetics and/or decrease the ligand off-loading from receptors. These enhancements appear to overcome the decrease induced by the increase in their molecular weights. Considering the above constraints, an increase in efficacy is directly related to the number of peptides attached to the carrier HPG molecule.

Chapter 5 – Conclusion

Here we address the some of the issues raised in the introduction and hypotheses regarding peptidomimetics, their conjugates, and anti-platelet inhibitor design: The RGD peptide has biological activity in the inhibition of GPIIbIIIa/fibrinogen interaction. The L -SHAYIGLKDR peptide has biological activity in the inhibition of GPIb-vWf interaction; its forward and reverse versions show similar activity while its D-enantiomers were found to have no inhibitory activity, which suggests that the inhibitory interaction is primarily orientation-, but not charge-dependent. These peptides do not cause spontaneous platelet activation as detected by CD62 surface expression/degranulation, GPIIbIIIa activation, compound light microscopy, and/or aggregometry. Conjugation to HPG through DVS functionalization of these peptides (RGD or SHAYIGLKDR) creates a biocompatible molecule/conjugate after the peptides are attached and the remaining VS groups are neutralized. HPG and HPG conjugated molecules do not cause spontaneous platelet activation macroscopically, or microscopically. Enhancement of peptide activity is observed to be linearly related to the number of molecules attached per HPG, within theoretical limits of peptide brush density, linker length, length of the pharmacophore, peptide chirality, peptide polarity, and the nature of the binding site interaction (linear vs internal). Peptide conjugation to HPG enhances peptide activity in a peptide-specific manner and increases the molecular weight of the peptide. This presents an excellent solution to the issues of low molecular weight, raised in the introduction with regards to peptidomimetics, and the same concepts can be widely applied to other molecules and are not limited to peptides.

In addition to the hypotheses, it must be reiterated that we have discovered a peptide that interferes with the GPIb-vWf interaction. This has important implications in drug design as conventional anti-platelet therapy tends to focus on downstream targets within platelet activation signalling pathways; this often results in inhibited platelets that have partially “spent” pathways and reduced activation potential upon further stimuli. A GPIb-vWf inhibitor can subvert this scenario as it targets one of the primary upstream targets of platelet activation, and hence serves as a superior anti-platelet therapeutic.

Bibliography

Agnelli G, Sonaglia F. (2002) Perspectives on antithrombotic agents: from unfractionated heparin to new antithrombotics. *Haematologica* 87: 757-770.

Andrews RK, Lopez JA, Berndt MC. (1997) Molecular mechanisms of platelet adhesion and activation. *The International Journal of Biochemistry and Cell Biology* 29: 91-105.

Bauer KA. (2006) New Anticoagulants. *Hematology / the education program of the American Society of Hematology* 6: 450-456.

Bearer EL, Prakash JM, Li Z. (2002) Actin dynamics in platelets. *International Review of Cytology* 217: 137-182.

Beer JH, Springer KT., Collier BS. (1992) Immobilized Arg-Gly-Asp (RGD) peptides of varying lengths as structural probes of the platelet glycoprotein IIb/IIIa receptor. *Blood* 79: 117-128.

Bjork I, Lindahl U. (1982) "Mechanism of the anticoagulant action of heparin". *Molecular and Cellular Biochemistry* 48: 161-182.

Boassavy JP, Sakariassen KS, Thalamas C, Boneu B, Cadroy Y. (1999) Antithrombotic efficacy of the vitamin K antagonist fluindione in a human *Ex vivo* model of arterial thrombosis: effect of anticoagulation level and combination therapy with aspirin. *Atherosclerosis, Thrombosis and Vascular Biology* 19: 2269-2275.

Bukow SC, Daffertshofer M, Hennerici MG. (2006) Tirofiban for the treatment of ischemic stroke. *Expert Opinion on Pharmacotherapy* 7: 73-79.

Bulmus V, Ding Z, Long CJ, Stayton PS, Hoffman AS. (2000) Site-specific polymer-streptavidin bioconjugate for pH-controlled binding and triggered release of biotin. *Bioconjugate Chemistry* 11: 78-83.

Calvete JJ. (2004) Structures of integrin domains and concerted conformational changes in the bidirectional signaling mechanism of $\alpha\text{IIb}\beta\text{3}$. *Experimental Biology and Medicine* 229: 732-744.

Castelli R, Cassinerio E, Cappellini MD, Porro E, Graziadei G, Fabris F. (2007) Heparin induced thrombocytopenia: pathogenic, clinical, diagnostic, and therapeutic aspects. *Cardiovascular and Haematological Disorders Drug Targets* 7: 153-162.

Chappell LT. (2007) Should EDTA chelation therapy be used instead of long-term clopidogrel plus aspirin to treat patients at risk from drug-eluting stents? *Alternative Medicine Reviews* 12: 152-158.

- Clementson KJ, Clementson JM. (2008) Platelet GPIb Complex as a target for anti-thrombotic drug development. *Thrombosis and Haemostasis* 99: 473-479.
- Coppinger JA, Maguire PB. (2007) Insights into the platelet releasate. *Current Pharmaceutical Design* 13: 2640-2646.
- Dawood BB, Wilde J, Watson SP. (2007) Reference curves for aggregation and ATP secretion to aid diagnose of platelet-based bleeding disorders: effect of inhibition of ADP and thromboxane A(2) pathways. *Platelets* 18: 329-345.
- del Caprio Munoz CA, Peissker T, Yoshimori A, Ichiishi E. (2003) Docking unbound proteins with MIAx: a novel algorithm for protein-protein soft docking. *Genome Informatics* 14: 239-249.
- del Caprio Munoz CA, Yoshimori A. (1999) MIAx: A novel system for assessment of macromolecular interaction in condensed phases. 1) Description of the interaction model and simulation algorithm. *Genome Informatics. Workshop on Genome Informatics* 10: 3-12.
- Du X. (2007) Signalling and regulation of the platelet GPIb-IX-V complex. *Current Opinion in Hematology* 14: 262-269.
- Dubois C, Steiner B, Meyer Reigner SC. (2004) Contribution of PAR-1, PAR-4 and GPIb α in intracellular signaling leading to the cleavage of the β 3 cytoplasmic domain during thrombin-induced platelet aggregation. *Thrombosis and Haemostasis* 91: 733-742.
- Farooqui AA, Taylor WA, Pendley CE, Cox JW, Horrocks LA. (2004) Spectrophotometric determination of lipases, lysophospholipases, and phospholipases. *Journal of Lipid Research* 25: 1555-156.
- Gabriel HM, Oliveira EI. (2006) Role of abciximab in the treatment of coronary artery disease. *Expert Opinion on Biological Therapy* 6: 935-46.
- Gibbins JM. (2004) Platelet adhesion signalling and the regulation of thrombus formation. *Journal of Cell Science* 117: 3415-3425.
- Gould R. (1994) The integrin α IIb β 3 as an antithrombotic. *Perspectives in Drug Discovery and Design* 1: 537-548.
- Grainger DW, Greef CH, Gong P, Lockhead MJ. (2007) Current microarray surface chemistries. *Methods in Molecular Biology* 381: 37-57.
- Grassetti DR, & Murray JF Jr. (1967) Determination of sulfhydryl groups with 2,2'- or 4,4'-dithiodipyridine. *Archives Biochemistry Biophysics* 119: 41- 49.

Green D. (2006) Coagulation Cascade. *Hemodialysis International. International Symposium on Home Dialysis* 10: Suppl 2, S2-S4.

Gupta AS, Huang G, Lestini BJ, Sagnella S, Kottke-Marchant K, Marchant RE. (2005) RGD-modified liposomes targeted to activated platelets as a potential vascular drug delivery system. *Journal of Thrombosis and Haemostasis* 93: 106-114.

Harrison P, Cramer EM. (1993) Platelet alpha granules. *Blood Reviews* 7: 52-62.

Hauptmann J. (2002) Pharmacokinetics of an emerging new class of Anticoagulant/antithrombotic drugs. *European Journal of Clinical Pharmacology* 57: 751-758.

Houen G, Jensen OM. (1995) Conjugation to Preactivated proteins using divinylsulfone and iodoacetic acid. *Journal of Immunological Methods* 181: 187-200.

Janssen APCA, Schiffelers RM, ten Hagenb TLM, Koninga GA, Schraac AJ, Kokc RJ, Storm G, Molemac G. (2003) Peptide-targeted PEG-liposomes in anti-angiogenic therapy. *International Journal of Pharmaceutics* 254: 55-58.

Joost A, Kurowski V, Radke PW. (2008) Anticoagulation in patients with heparin-induced thrombocytopenia undergoing percutaneous coronary angiography and interventions. *Current Pharmaceutical Design* 14: 1176-1185.

Jurk K, Kehrel BE. (2005) Platelets: physiology and biochemistry. *Seminars in Thrombosis and Haemostasis* 31: 381-392.

Juttler E, Kohrmann M, Schellinger PD. (2006) Therapy for early reperfusion after stroke. *Nature Clinical Practice* 3: 656-663.

Kainthan RK, Mulawan EB, Hatzikiriakos SG, Brooks DE. (2006) Synthesis, characterization, and viscoelastic properties of high molecular weight branched polyglycerols. *Macromolecules* 39: 7708-7717.

Kainthan RK, Hester SR, Levin E, Devine DV, Brooks DE. (2007) *In vitro* biological evaluation of high molecular weight hyperbranched polyglycerols. *Biomaterials* 28: 4581-4590.

Kainthan RK, Brookes DE. (2007) *In vivo* biological evaluation of high molecular weight hyperbranched polyglycerols. *Biomaterials* 28: 4779-4787.

Kasirer-Friede A, Legrand C, Frojmovic MM. (2001) Complementary roles for fibrin(ogen), thrombospondin and vWF in mediating shear-dependent aggregation of platelets stimulated at threshold thrombin concentrations. *Thrombosis and Haemostasis* 86: 653-659.

- Katira R, Chauhan A, More RS. (2005) Direct thrombin inhibitors: novel antithrombotics on the horizon in the thromboprophylactic management of atrial fibrillation. *Postgraduate Medical Journal* 81: 370-375.
- Kaushansky K. (2005) The molecular mechanisms that control thrombopoiesis. *Journal of Clinical Investigation* 115: 3339-3347.
- Kim W. J., Yockman J. W., Jeong J. H., Christensen L. V., Lee M., Kim Y. H., Kim S. W. (2005) Soluble Flt-1 gene delivery using PEI-g-PEG-RGD conjugate for anti-angiogenesis. *Journal of Controlled Release* 106: 224-234.
- Kirchmaier AL, Sugden B. (1997) Dominant-Negative Inhibitors of EBNA-1 of Epstein-Barr virus. *Journal of Virology* 71: 1766-1775.
- Knischka R., Lutz PJ, Sunder A, Mülhaupt R. Frey H. (2000) Functional poly(ethylene oxide) multiarm star polymers: Core-first synthesis using hyperbranched polyglycerol initiators. *Macromolecules* 33: 315-320.
- Lee I, Marchant RE. (2003) Molecular interaction studies of hemostasis: fibrinogen ligand-human platelet receptor interactions. *Ultramicroscopy* 97: 341-352.
- Linkins LA, Warkentin TE. (2008) The approach to heparin induced thrombocytopenia. *Seminars in Respiratory and Critical Care Medicine* 29: 66-74.
- Lopez JA, Dong JF. (2005) Shear stress and the role of high molecular weight von Willebrand factor multimers in thrombus formation. *Blood Coagulation and Fibrinolysis: An International Journal in Haemostasis and Thrombosis* 16: Suppl 1, S11-S16.
- Mason KD, Carpinelli MR, FletcherJI, Collinge JE, Hilton AA, Ellis S, Kelly PN, Ekert PG, Metcalf D, Roberts AW, Huang DC, Kile BT. (2007) Programmed anuclear cell death delimits platelet life span. *Cell* 128: 1173-1186.
- McGregor L, Martin J, McGregor JL. (2006) Platelet-leukocyte aggregates and derived microparticles in inflammation, vascular remodelling and thrombosis. *Frontiers in Bioscience: A Journal and Virtual Library* 11: 830-837.
- McRae SJ, Ginsberg JS. (2005) New anticoagulants for the prevention and treatment of venous thromboembolism. *Vascular Health Risk Management* 1: 41-53.
- Merli GJ, Fink J. (2008) Vitamin K and thrombosis. *Vitamins and Hormones* 78: 265-279.
- Mousa SA, Bozarth JM, Naik UP, Slee A. (2001) Platelet GPIIb/IIIa binding characteristics of small molecule RGD mimetic: distinct binding profile for Roxifiban. *British Journal of Pharmacology* 133: 331-336.

Mosesson MW. (2005) Fibrinogen and fibrin structure and functions. *Journal of Thrombosis and Haemostasis* 3: 1894-1904.

Nicholson NS, Panzer-Knodel SG, Salyers AK, Taite BB, King LW, Miyano M, Gorczynski RJ, Williams MH, Zupec ME, Tjoeng FS. (1991) *In vitro* and *in vivo* effects of a peptide mimetic (SC-47643) of RGD as an antiplatelet and antithrombotic agent. *Thrombosis Research* 62: 567-78.

Niitsu Y, Jakubowski JA, Sugidachi A, Asai F. (2005) Pharmacology of CS-747 (Prasugrel, LY640315), novel, potent antiplatelet agent with *in vivo* P₂Y₁₂ receptor antagonist activity. *Seminars in Thrombosis and Haemostasis* 31: 184-194.

Ojima I, Chakravarty S, Dong Q. (1995) Antithrombotic agents: from RGD to peptide mimetics. *Bioorganic & Medicinal Chemistry* 3: 337-360.

Prandoni P, Tormene D, Perlati M, Brandolin B, Spiezia L. (2008) Idraparinux: review of its clinical efficacy and safety for prevention and treatment of thromboembolic disorders. *Expert Opinion on Investigational Drugs* 17: 773-777.

Reiner CK, Kada G, Grubber HJ. (2002) *Analytical and Bioanalytical Chemistry* 373: 266-276.

Ruggeri ZM. (2007) The role of von Willebrand factor in thrombus formation. *Thrombosis Research* 120 Suppl 1: S5-S9.

Ruoslahti E, Pierschbacher MD. (1987) New perspectives in cell adhesion: RGD and integrins *Science* 238: 491 – 497.

Selwyn AP. (2003) Prothrombotic and antithrombotic pathways in acute coronary syndromes. *The American Journal of Cardiology* 19: 3H-11H.

Shattil SJ, Newman PJ. (2004) Integrins: dynamic scaffolds for adhesion and signaling in platelets. *Blood* 104: 1606-1615.

Sheu JR., Huang TF. (1994) Ex-vivo and in-vivo antithrombotic effect of triflavin, an RGD-containing peptide. *Journal of Pharmacy and Pharmacology* 46: 58-62.

Sunder A, Mulhaupt R, Frey H. (2000) Hyperbranched polyether-polyols based on polyglycerol: polarity design by block copolymerization with propylene oxide *Macromolecules* 33: 309-314.

Sunder A, Heinemann J, Frey H. (2000) Controlling the growth of polymer trees: concepts and perspectives for hyperbranched polymers. *Chemistry* 6: 2499-2506.

- Temming K, Lacombe M, Schaapveld RQ, Orfi L, Kéri G, Poelstra K, Molema G, Kok R J (2006) Rational design of RGD-albumin conjugates for targeted delivery of the VEGF-R kinase inhibitor PTK787 to angiogenic endothelium. *ChemMedChem* 1: 1200 – 1203.
- Urban JJ, Tillman BG, Cronin WA. (2006) Fluoroolefins as peptide mimics: a computational study of structure, charge distribution, hydration, and hydrogen bonding. *Journal of Physical Chemistry* 110: 11120-11129.
- Vanhoorelbeke K, Ulrichs H, Schoolmeester A, Deckmyn H. (2003) Inhibition of platelet adhesion to collagen as a new target for antithrombotic drugs. *Current Drug Targets. Cardiovascular and Haematological Disorders* 3:125-140.
- Varga-Szabo D, Pleines I, Nieswandt B. (2008) Cell adhesion mechanisms in platelets. *Arteriosclerosis, Thrombosis, and Vascular Biology* 28: 403-412.
- Vilahur G, Casani L, Badimon L. (2007) A thromboxane A₂/prostaglandin H₂ receptor antagonist (S18886) shows high antithrombotic efficacy in an experimental model of stent-induced thrombosis. *Thrombosis and Haemostasis* 98: 662-669.
- Walensky LD, Kung AL, Esche I, Malia TJ, Barbuto S, Wright RD, Wagner G, Verdine GL, Korsmeyer SJ, (2004) Activation of apoptosis in vivo by a hydrocarbon-stapled BH3 helix. *Science* 3: 1466-1470.
- Walsh GM, Sheehan D, Kinsella A, Moran N, O'Neil. (2004) Redox modulation of integrin [correction of integin] α IIb β 3 involves a novel allosteric regulation of its thiol isomerase activity. *Biochemistry* 43: 473-480.
- Watson HG, Chee YL. (2008) Aspirin and other anti-platelet drugs in the prevention of venous thromboembolism. *Blood Reviews* 22: 107-116.
- Watson SP, Auger JM, McCarty OJ, Pearce AC. (2005) GPVI and integrin α IIb β 3 signaling in platelets. *Journal of Thrombosis and Haemostasis* 3: 1752-1762.
- Wiley RA, Rich DH. (1993) Peptidomimetics derived from natural products. *Medical Research Reviews* 13: 327-384.
- Yasuda O, Takemura Y, Kawamoto H, Rakugi H. (2008) Aspirin: Recent developments. *Cellular and Molecular Life Sciences* 65: 354-358.
- Yin H, Liu J, Li Z, Berndt MC, Lowell CA, Du X. (2008) Src family tyrosine kinase Lyn mediates VWF/GPIb-IX-induced platelet activation via the cGMP signaling pathway. *Blood*, Epub June 11.
- Yoshimori A, del Caprio Munoz CA. (2001) Automatic epitope recognition in proteins oriented to the system for macromolecular interaction assessment MIAx. *Genome Informatics. International Conference on Genome Informatics* 12: 113-121.

Zeymer U, Wienbergen H. (2007) A review of clinical trials with eptifibatide in cardiology. *Cardiovascular Drug Reviews* 25: 301-315.


Zhang JG, Krajden OB, Kainthan RK, Kizhakkedathu JN, Constantinescu I, Brooks DE, Gyongyossy-Issa MIC. (2008) Conjugation to hyperbranched polyglycerols improves RGD-mediated inhibition of platelet function *in vitro*. *Bioconjugate Chemistry* 19: 1241-1247.

Zimmerman GA, Weyrich AS. (2008) Signal-dependent protein synthesis by activated platelets: new pathways to altered phenotype and function. *Arteriosclerosis, Thrombosis, and Vascular Biology* 28: s17-24.

Appendices

Appendix A

UBC Research Ethics Board Approval Certificate

 The University of British Columbia Office of Research Services Clinical Research Ethics Board - Room 210, 828 West 10th Avenue, Vancouver, BC V5Z 1L8						
ETHICS CERTIFICATE OF EXPEDITED APPROVAL: RENEWAL						
PRINCIPAL INVESTIGATOR: Maria Issa	DEPARTMENT: UBC/Medicine, Faculty of Pathology & Laboratory Medicine	UBC CREB NUMBER: 403-70559				
INSTITUTION(S) WHERE RESEARCH WILL BE CARRIED OUT:						
<table border="1"><thead><tr><th>Institution</th><th>Site</th></tr></thead><tbody><tr><td>UBC</td><td>Vancouver (excludes UBC Hospital)</td></tr></tbody></table>			Institution	Site	UBC	Vancouver (excludes UBC Hospital)
Institution	Site					
UBC	Vancouver (excludes UBC Hospital)					
Other locations where the research will be conducted: Canadian Blood Services - Network Centre for Applied Development where, in some cases, the blood will be drawn. In most cases, blood will be drawn at the LSI Research Blood Collection Suite.						
CO-INVESTIGATOR(S): Ken Scammel Catherine Walsh J Zhang Katherine Serrano Elena Levin Juergen Keat Sandra Weiss Irina Constantinescu Cheryl Pittendrigh Nobu Kikuchi Peter Schubert Elizabeth Maurer Faith Hunter Jonathan Thon Brankica Culibrk Dana V. Downie						
SPONSORING AGENCIES: Canadian Blood Services - "General Instrument Calibration and Reference Material"						
PROJECT TITLE: Human Blood for General Instrument Calibration, Reference Material and Reagent						

EXPIRY DATE OF THIS APPROVAL: **January 28, 2009**

APPROVAL DATE: **January 28, 2008**

CERTIFICATION

In respect of clinical trials:

1. The membership of this Research Ethics Board complies with the membership requirements for Research Ethics Boards defined in Division 5 of the Food and Drug Regulations.
2. The Research Ethics Board carries out its functions in a manner consistent with Good Clinical Practices.
3. The Research Ethics Board has reviewed and approved the clinical trial protocol and informed consent form for the trial which is to be conducted by the qualified investigator named above at the specified clinical trial site. This approval and the views of this Research Ethics Board have been documented in writing.

The Chair of the UBC Clinical Research Ethics Board has reviewed the documentation for the above named project. The research study, as presented in the documentation, was found to be acceptable on ethical grounds for research involving human subjects and was approved for renewal by the UBC Clinical Research Ethics Board.

Approval of the Clinical Research Ethics Board by

Dr. James McCormack, Associate Chair